

Co-Editor Decision: Reconsider after major revisions (23 Sep 2016) by Dr. Jens-Uwe Grooß

We thank Dr. Grooß for the insightful comments. Below we provide a detailed point-by-point answer (AC – Author Comment) to each comment on our manuscript (CEC – Co-Editor Comment).

CEC:

Comments to the Author:

Dear authors,

In my impression, you should have considered more of the reviewers comments. So please consider the remaining points expressed by the two reviewers as well as the following technical points:

Title: "after dark" means to my knowledge something like "after it did get dark". It could be mis-understood as "after the dark period", which would be at morning. You also mention the peak at sunrise, so I also would prefer to be the title as suggested by reviewer #1 ("Nighttime Iodine chemistry" or so.)

AC:

We have changed the title to “Nighttime atmospheric chemistry of iodine”.

CEC:

"buildup of HOI"

In your figure 4 (HOI scenario 1) HOI is clearly decreasing during night and it is not building up, although the shown HOI emissions are increasing. You could likely visualize the nighttime values better, if the used colour label differences would not be linear, but e.g. logarithmic. But in the text should be clarified, that part of the emitted HOI has a faster or slower sink depending on scenario.

AC:

We have corrected that statement in the manuscript (page 13, lines from 6 to 9)

CEC:

**"which is converted into I₂/IBr/ICl through heterogeneous recycling" (2 times)
What do you mean by that? According to your reaction list in the attachment there
the HOI would react to IBr/ICl on the aerosols but not to I₂.**

AC:

Thanks!. You are right; we have corrected it and replaced "I₂/IBr/ICl" by "IBr/ICl".

CEC:

**"Figures 4 and 5" please use "local time" a x-coordinate as suggested by the
reviewer and mention the two-day spin-up elsewhere.**

AC:

We have replaced "Time" by "Local time" in x-axis labels, and mentioned "after two
days of simulation time" in the text (P13, L2 and P13, L18).

CEC:

**"Figure 4 middle right" please do not truncate the colour labels of the contour
plot.**

AC:

Labels have been replaced by a color scale.

CEC:

**"Figure 5": please use also IONO₂ instead of INO₃ in the bottom panels to be
consistent with the text.**

AC:

corrected

CEC:

**"Figure 6": please explain in more detail which NO₃ value is plotted (certain local
time, average nighttime or what).**

AC:

We now mention in the text (P14, L16) and in the caption of figure 6 that it refers to
NO₃ peak nighttime concentration.

CEC:

"figure 7-9, colour bar label" use (greek) Delta HOI and Delta I2 as you show a difference.

AC:

Thank you for the suggestion. We have now included the Delta in the label of the three figures.

Non-public comments to the Author:

Dear authors,

thank you for submitting the revised version. Since I am not an expert in modelling at the molecular level, I asked Florent Louis and one other reviewer to look, whether their comments have been answered sufficiently. As you see, they still have some points, which I would ask you to consider.

regards, Jens-Uwe Grooß

Anonymous Referee #1

We thank the reviewer for his/her insightful comments. Below we provide a detailed point-by-point answer (AC – Author Comment) to each comment on our manuscript (RC – Reviewer Comment).

Suggestions for revision or reasons for rejection (will be published if the paper is accepted for final publication)

In my opinion, the scientific content of the revised version of the manuscript is sufficient to justify publication in ACP. Unfortunately, however, the authors ignored several suggestions from the reviewers to improve the presentation quality which is also important for a high-quality article. In particular, I would like to reiterate the following points:

RC:

Thank you for showing the iodine reaction mechanism in the supplement. You mention that the scheme is referenced in page 22 line 12 in the main text but I cannot find it there. Although the supplement now shows all iodine reactions, the non-iodine reactions in the model are still not listed. For example, IO + BrO is listed but BrO + BrO is not listed, even though this reaction will also have an indirect effect on reactive iodine concentrations.

AC:

You are correct, supplementary information is referenced in page 5 line 10. Now, we have also cited, in the same page and line, the work of Ordoñez et al., 2012, which includes all iodine and non-iodine reactions included in the model. We think that it would be redundant to include the same supplement that has already been included in Ordoñez et al., 2012.

RC:

I know that LT refers to local time. However, this may not be clear to all readers. I think that all acronyms should be explained in the text when they are used for the first time.

AC:

Acronym LT (Local Time) has now been defined in Page 15, line 1.

RC:

It may be customary to quote vibrational frequencies as wave numbers but it is incorrect. It is like saying "the frequency of green light is 500 nm".

AC:

Although it may be incorrect, this is the conventional units for vibrational frequency which is accepted by the community. So we respectfully prefer to keep table 2 in its current form.

RC:

Provided that enough significant digits are shown, it is fine to show the numbers in the plots of Figs. 4 and 5 instead of using a color scale. Nevertheless, I still find it confusing if two plots in the same row use slightly different color schemes. It makes a comparison unnecessarily complicated.

AC:

Thanks for the suggestion. We have now replaced figures 4 and 5 by new ones including the same colour scale.

RC:

The information that "nighttime" refers to the average between midnight and 01:00 local time is important and should be shown in the figure caption. If you want to avoid repetition, it could be removed from the text.

AC:

(from 0:00 to 1:00 LT) has been included in the figure captions.

RC:

The effect of the new chemistry on DMS is quite indirect. You mention that DMS changes because of NO₃. In addition, the new iodine chemistry will most probably also affect bromine chemistry, and different BrO will also affect DMS concentrations. I think that either this should also be discussed, or figure 9 should be removed, as another reviewer had suggested.

AC:

The effect of this iodine chemistry on bromine is negligible, so we would expect a direct effect on DMS through NO_3 . Therefore we respectfully prefer to keep figure 9 in the manuscript.

Referee #4: LOUIS, Florent

Interactive comment on “Iodine chemistry after dark” by Alfonso Saiz-Lopez et al.

We thank Dr. Louis for the insightful comments. Below we provide a detailed point-by-point answer (AC – Author Comment) to each comment on our manuscript (RC – Referee Comment).

RC:

I posted an interactive comment on "Iodine chemistry after dark" by Saiz-Lopez et al. on July 4th 2016. This paper represents a very important contribution dealing with atmospheric iodine chemistry. I made several comments. There is still one comment for which the authors do not take into account my recommendation.

It concerns the spin-orbit correction (SOC) for iodine-containing species involved in the studied reactions. I previously reported "The authors stated on page 6 line 12 that "spin-orbit splittings of -17 and -5 kJ mol⁻¹ were applied to energies of I and IO". These values do not correspond to the well known value for I atom (-30.3 kJ mol⁻¹ from C.E. Moore, Atomic Energy Levels, USGPO, Vols. II and III. NSRDS-NBS 35, Washington, DC, 1971). Over the last years, my group performed theoretical calculations to get the SOC values for numerous iodine-containing species using the CASPT2/RASSI methodology. The corresponding values for I, IO, and HOI are -30.0, -14.4, and -5.9 kJ/mol (Meciarova et al., CPL, 2011, 517, 149; Khanniche et al., JPCA, 2016, 120, 1737; Sulkova et al., JPCA, 2013, 117, 771). These calculations were also validated by comparison to few available data. I recommend the authors to update their energetics according to the correct SOC values".

There are large differences between SOC values for I and IO (-17 and -5 kJ mol⁻¹) in the manuscript and the literature data (-30 and -14 kJ mol⁻¹). I would expect the authors will revise their energetics according to the most reliable data. Kinetic parameters should be also re-evaluated.

AC:

We have followed the reviewer's suggestion and included these recent spin-orbit corrections in the calculated reaction energetics of the three reactions. For reaction 4, the estimated rate coefficient remains unchanged, although k_4 is possibly a lower limit because of the increasing spin-orbit correction across the potential surface from HOI to IO. This is now discussed in the following changes in Section 3 of the paper (page 6, line 11 to page 7, line 11):

“Spin-orbit corrections of -30.0 (Mečiarová et al., 2011), -14.4 (Khanniche et al., 2016), -5.9 (Šulková et al., 2013) and -4.8 (Kaltsoyannis and Plane, 2008) kJ mol⁻¹ were applied to the energies of I, IO, HOI and IONO₂, respectively.

Reaction 2 is endothermic by 2.6 kJ mol⁻¹ and so, within the expected error of ± 10 kJ mol⁻¹ at this level of theory, might be reasonably fast. However, the transition state of the reaction, which is illustrated in Figure 2(a), is 73 kJ mol⁻¹ above the reactants and so this reaction will not occur at tropospheric temperatures. Reaction 3 is exothermic by 19.8 kJ mol⁻¹. An HOI--HNO₃ complex first forms (Figure 2(b)), which is 21 kJ mol⁻¹ below the reactants. However, this complex re-arranges to the IONO₂ + H₂O products via the cyclic transition state shown in Figure 2(c), which is 110 kJ mol⁻¹ above the reactants.

The stationary points on the potential energy surface (PES) for reaction 4 are illustrated in Figure 3. HOI and NO₃ associate to form a complex which is 24 kJ mol⁻¹ below the reactant entrance channel. H-atom transfer involves a submerged transition state to form an IO--HNO₃ complex, which can then dissociate to the products IO + HNO₃. The vibrational frequencies, rotational energies and geometries (in Cartesian co-ordinates) of these intermediates are listed in Table 2. Overall, the reaction is exothermic by 14 kJ mol⁻¹. The energies of the HOI--NO₃ complex and the transition state are assigned the same spin-orbit correction as HOI (-5.9 kJ mol⁻¹ (Šulková et al., 2013)), whereas the IO--HNO₃ complex is assigned the spin-orbit correction of IO (-14.4 kJ mol⁻¹ (Khanniche et al., 2016)). This reflects the H-OI bond only increasing from 0.97 Å in HOI to 1.1 Å in the transition state, compared with 1.7 Å in the IO—HNO₃ complex. The spin-orbit correction for the transition state is therefore likely to be closer to that of HOI. Assigning the HOI spin-orbit correction therefore means that the barrier is highest with respect to the reactants, so that the estimated rate coefficient (see below) may be a lower limit.”

page 8, line 23 to page 9, line 10:

“The uncertainty in k_4 arises principally from the estimated capture rate coefficient (see above), and the height of the barrier below the entrance channel. As discussed above, the spin-orbit correction of the transition state is likely to be larger than the value of -5.9 kJ mol⁻¹ corresponding to HOI, so k_4 is possibly a lower limit. For instance, if the barrier height is decreased by 3 kJ mol⁻¹, k_4 increases by a factor of 1.9. If the barrier is lower by 8.5 kJ mol⁻¹ (corresponding to the transition state having the same spin-orbit correction as IO), then k_4 would increase by a factor of 5.1. Nevertheless, noting that the capture rate coefficient could be lower – perhaps by a factor of 2 - than the estimate used here, we prefer to use the value for k_4 calculated with the potential surface in Figure 3. Of course, if k_4 is larger, then the atmospheric impacts of reaction 4 discussed in Section 4 will be even more pronounced.”

RC:

For the second comment dealing with the treatment of low frequency modes in the intermediate species, I would suggest the authors to mention only in the

manuscript : "The rigid-rotor harmonic oscillator approximation has been used for all species". Hindered rotor treatment for low frequency modes could influence the entropy contribution. Of course, it will depend on the rotational barrier height, its periodicity and the model used. It is often used without any available experimental data.

AC:

We have adopted this suggestion (page 7, line 23).

RC:

Other comments have been properly answered by the authors.

1 | **Nighttime atmospheric chemistry of iodine** ~~after dark~~

2 | Alfonso Saiz-Lopez¹, John M.C. Plane², Carlos A. Cuevas¹, Anoop S. Mahajan³, Jean-François
3 | Lamarque⁴ and Douglas E. Kinnison⁴

4 | ¹Department of Atmospheric Chemistry and Climate, Institute of Physical Chemistry
5 | Rocasolano, CSIC, Madrid, Spain

6 |
7 | ²School of Chemistry, University of Leeds, Leeds, UK

8 |
9 | ³Indian Institute of Tropical Meteorology, Pune, India

10 |
11 | ⁴Atmospheric Chemistry Observations and Modelling, NCAR, Colorado, USA

12 | Correspondence to: A. Saiz-Lopez (a.saiz@csic.es)

1 **Abstract**

2 Little attention has so far been paid to the nighttime atmospheric chemistry of iodine species.
3 Current atmospheric models predict a buildup of HOI and I₂ during the night that leads to a spike
4 of IO at sunrise, which is not observed by measurements. In this work, electronic structure
5 calculations are used to survey possible reactions that HOI and I₂ could undergo at night in the
6 lower troposphere, and hence reduce their nighttime accumulation. The new reaction NO₃ + HOI
7 → IO + HNO₃ is proposed, with a rate coefficient calculated from statistical rate theory over the
8 temperature range 260 - 300 K and at a pressure of 1000 hPa to be $k(T) = 2.7 \times 10^{-12} (300 \text{ K} / T$
9 $)^{2.66} \text{ cm}^3 \text{ molecule}^{-1} \text{ s}^{-1}$. This reaction is included in two atmospheric models, along with the
10 known reaction between I₂ and NO₃, to explore a new nocturnal iodine radical activation
11 mechanism. The results show that this iodine scheme leads to a considerable reduction of
12 nighttime HOI and I₂, which results in the enhancement of more than 25% of nighttime ocean
13 emissions of HOI + I₂ and the removal of the anomalous spike of IO at sunrise. We suggest that
14 active nighttime iodine can also have a considerable, so far unrecognized, impact on the
15 reduction of the NO₃ radical levels in the marine boundary layer (MBL) and hence upon the
16 nocturnal oxidizing capacity of the marine atmosphere. The effect of this is exemplified by the
17 indirect effect on dimethyl sulfide (DMS) oxidation.

18

19

20

21

1 **1. Introduction**

2 Active nighttime iodine chemistry was first evidenced a decade ago when it was shown that
3 nocturnal I₂ emitted by macroalgae could react with NO₃ leading to the formation of IO and
4 OIO, which were measured in the coastal MBL at Mace Head, Ireland (Saiz-Lopez and Plane,
5 2004). The nitrate radical has also been recently suggested as a nocturnal loss of CH₂I₂, which
6 helps to reconcile observed and modelled concentrations of this iodocarbon over the remote
7 MBL (Carpenter et al., 2015). However, most of the work on reactive atmospheric iodine has
8 focused on the use of daytime observations and models to assess its role in the catalytic
9 destruction of ozone and the oxidizing capacity of the troposphere (e.g. Saiz-Lopez et al. (2012b)
10 and references therein). In the MBL, iodine-, along with bromine-catalysed ozone destruction
11 contributes up to 45% of the observed daytime depletion (Read et al., 2008; Mahajan et al.,
12 2010a), although this contribution shows large geographical variability (Mahajan et al., 2012;
13 Gómez Martín et al., 2013; Prados-Roman et al., 2015b; Volkamer et al., 2015). Iodine
14 compounds have also been implicated in the formation of aerosols, although the mechanisms and
15 magnitudes of these processes are not fully understood (Hoffmann et al., 2001; O'Dowd et al.,
16 2002; McFiggans et al., 2004; Gomez Martin et al., 2013; Allan et al., 2015; Roscoe et al., 2015).
17 Reactive forms of inorganic iodine may also contribute to the oxidation of elemental mercury
18 over the tropical oceans (Wang et al., 2014). In recent years, iodine sources and chemistry have
19 also been implemented in global models demonstrating the effect of iodine chemistry in the
20 oxidation capacity of the global marine troposphere (Ordóñez et al., 2012; Saiz-Lopez et al.,
21 2012a; Saiz-Lopez et al., 2014; Sherwen et al., 2016).

22 Iodine is emitted into the atmosphere from the ocean surface in both organic and inorganic
23 forms. The main organic compounds emitted are methyl iodide (CH₃I), ethyl iodide (C₂H₅I),

1 propyl iodide (1- and 2-C₃H₇I), chloriodomethane (CH₂ICl), bromiodomethane (CH₂IBr), and
2 diiodomethane (CH₂I₂) (Carpenter, 2003; Butler et al., 2007; Jones et al., 2010; Mahajan et al.,
3 2012). However, these organic compounds contribute only up to a fourth of the MBL iodine
4 loading (Jones et al., 2010; Mahajan et al., 2010a; Großmann et al., 2013; Prados-Roman et al.,
5 2015b). Inorganic emissions of HOI and I₂, which result from the deposition of O₃ at the ocean
6 surface and subsequent reaction with I⁻ ions in the surface microlayer, account for the main
7 source of iodine in the MBL (Carpenter et al., 2013). Recent laboratory experiments have shown
8 that HOI is the major compound emitted, and provided parameterizations of the fluxes of both
9 species depending on wind speed, temperature, and the concentrations of O₃ and I⁻ (Carpenter et
10 al., 2013; MacDonald et al., 2014). These parameterized fluxes of HOI and I₂ have then been
11 used in a one-dimensional model to study the diurnal evolution of the IO and I₂ mixing ratios at
12 the Cape Verde Atmospheric Observatory (CVAO) (Carpenter et al., 2013; Lawler et al., 2014).
13 The model simulations replicate well the levels and general diurnal profiles of IO and I₂,
14 although an early morning ‘dawn spike’ in IO is predicted by the models, but has not been
15 observed (Read et al., 2008; Mahajan et al., 2010a). The morning peak predicted by current
16 iodine chemistry models is due to a buildup of the emitted I₂ and HOI (which is converted into
17 I₂/IBr/ICl through heterogeneous sea-salt recycling) over the course of the night, followed by
18 rapid photolysis at sunrise.

19 Traditionally it has been thought that iodine chemistry has a negligible effect on oxidizing
20 capacity of the nocturnal marine atmosphere. As a consequence, unlike the demonstrated effect
21 of iodine on the levels of daytime oxidants, the impact of active iodine upon the main nighttime
22 oxidant, NO₃, remains an open question. This is important given that in many parts of the ocean
23 the NO₃ + DMS reaction is at least as important as OH + DMS in oxidizing DMS (Allan et al.,

1 2000), and hence a reduction of NO₃ may have an effect in the production of SO₂ and methane
2 sulfonic acid (MSA). Here, we discuss possible mechanisms of nighttime iodine radical
3 activation and their potential effect on nighttime iodine ocean fluxes and the currently modeled
4 dawn spike in IO. A new reaction of HOI with NO₃ is proposed, supported by theoretical
5 calculations. We explore the implications of this new reaction both for iodine and NO₃
6 chemistries.

7

8 **2. Nocturnal iodine radical activation mechanism**

9 We use the reaction mechanism that has recently been described in [the a](#)-global modelling
10 [stud](#)[iesy](#) by Saiz-Lopez et al. (2014) [and](#) (Ordóñez et al., 2012) (see supplementary information).

11 In addition to the reactions included in that scheme, we also include nighttime gas-phase
12 reactions based on the theoretical calculations described below. The additional reactions are
13 listed in Table 1 and a scheme with this new nocturnal chemistry is included in Figure 1.

14 To the best of our knowledge, reactions of HOI specific to night time have not been studied,
15 either theoretically or through laboratory experiments. Currently, HOI is thought to build up
16 overnight until sunrise, with only heterogeneous uptake on seasalt aerosol as a nighttime loss
17 process (Saiz-Lopez et al., 2012b; Simpson et al., 2015). In addition to the well known I₂ + NO₃
18 reaction (R1) (Chambers et al., 1992), here we consider several possible HOI reactions that could
19 occur at night, in the absence of photolysis and OH:





2

3 **3. Theoretical calculations**

4 In order to explore the feasibility of reactions 2–4 taking place under the conditions of the lower
5 troposphere, we carried out electronic structure calculations using the hybrid density
6 functional/Hartree-Fock B3LYP method from within the Gaussian 09 suite of programs (Frisch
7 et al., 2009), combined with a G2 level basis set for I (Glukhovtsev et al., 1995) and the standard
8 6-311+g(2d,p) triple zeta basis set for O, N and H. Following geometry optimizations of the
9 relevant points on the potential energy surfaces, and the determination of their corresponding
10 vibrational frequencies and (harmonic) zero-point energies, energies relative to the reactants
11 were obtained at the same level of theory. Spin-orbit corrections of -30.0 (Mečiarová et al.,
12 2011), -14.417 (Khanniche et al., 2016), ~~and -5.9~~ (Šulková et al., 2013) and -4.8 (Kaltsoyannis
13 and Plane, 2008) kJ mol^{-1} were applied to the energies of I₂, ~~and IO₂~~, HOI and IONO₂,
14 ~~respectively~~, ~~(Šulková et al., 2013)~~; ~~these were estimated by comparing the theoretical and~~
15 ~~experimental bond energies of I₂ and IO, calculated at the level of theory used in the present~~
16 ~~study, with available experimental data (Plane et al., 2006; Kaltsoyannis and Plane, 2008).~~

17 Reaction 2 is endothermic by 2.69 kJ mol^{-1} and so, within the expected error of $\pm 10 \text{ kJ mol}^{-1}$ at
18 this level of theory, might be reasonably fast. However, the transition state of the reaction, which
19 is illustrated in Figure 2(a), is 73 kJ mol^{-1} above the reactants and so this reaction will not occur
20 at tropospheric temperatures. Reaction 3 is exothermic by 19.811 kJ mol^{-1} . An HOI--HNO₃
21 complex first forms (Figure 2(b)), which is 21 kJ mol^{-1} below the reactants. However, this

1 complex re-arranges to the $\text{IONO}_2 + \text{H}_2\text{O}$ products via the cyclic transition state shown in Figure
2 2(c), which is 110 kJ mol^{-1} above the reactants.

3 The stationary points on the potential energy surface (PES) for reaction 4 are illustrated in Figure
4 3. HOI and NO_3 associate to form a complex which is 24 kJ mol^{-1} below the reactant entrance
5 channel. H-atom transfer involves a submerged transition state to form an IO-- HNO_3 complex,
6 which can then dissociate to the products IO + HNO_3 . The vibrational frequencies, rotational
7 energies and geometries (in Cartesian co-ordinates) of these intermediates are listed in Table 2.

8 Overall, the reaction is exothermic by ~~14~~ 141 kJ mol^{-1} . The energies of the HOI-- NO_3 complex and
9 the transition state are assigned the same spin-orbit correction as HOI (-5.9 kJ mol^{-1} (Šulková et
10 al., 2013)), whereas the IO-- HNO_3 complex is assigned the spin-orbit correction of IO (-14.4 kJ
11 mol^{-1} (Khanniche et al., 2016)). This reflects the H-OI bond only increasing from 0.97 \AA in HOI
12 to 1.1 \AA in the transition state, compared with 1.7 \AA in the IO-- HNO_3 complex. The spin-orbit
13 correction for the transition state is therefore likely to be closer to that of HOI. (Khanniche et al.,
14 2016) Assigning the HOI spin-orbit correction therefore means that the barrier is highest with
15 respect to the reactants, so that the estimated rate coefficient (see below) may be a lower limit.
16 ~~The vibrational frequencies, rotational energies and geometries (in Cartesian co-ordinates) of~~
17 ~~these intermediates are listed in Table 2.~~

18 The rate coefficient for reaction 4 was then estimated using Rice-Ramsperger-Kassel-Markus
19 (RRKM) theory, employing a multi-well energy-grained master equation solver based on the
20 inverse Laplace transform method - MESMER (Master Equation Solver for Multi-well Energy
21 Reactions) (Roberston et al., 2014). The reaction proceeds via the formation of the excited
22 HOI-- NO_3 complex from HOI + NO_3 . This complex can then dissociate back to the reactants or
23 rearrange to the IO-- HNO_3 intermediate complex over the transition state, which can in turn

1 dissociate to the products IO + HNO₃. Either of the intermediates can also be stabilized by
2 collision with the third body (N₂). The time evolution of all these possible outcomes is modelled
3 using the master equation.

4 The internal energies of the intermediates on the PES were divided into a contiguous set of
5 grains (width 10 cm⁻¹), each containing a bundle of rovibrational states calculated with the
6 molecular parameters in Table 2, [using the rigid-rotor harmonic oscillator approximation for all](#)
7 [species](#). It should be noted that the HOI--NO₃ and IO--HNO₃ complexes both have low
8 frequency vibrational modes (< 100 cm⁻¹) which should more correctly be treated as hindered
9 rotors rather than vibrations. However, in our experience this is not worth doing this until
10 experimental rate coefficients are available to fit the rotor barrier heights. In any case, the
11 energies of both complexes are far enough below the energy of the entrance channel (figure 3)
12 that relatively small changes in their densities of states will have a minor effect on the overall
13 rate coefficient. Each grain was then assigned a set of microcanonical rate coefficients linking it
14 to other intermediates, calculated by RRKM theory. For dissociation to products or reactants,
15 microcanonical rate coefficients were determined using inverse Laplace transformation to link
16 them directly to the capture rate coefficient, k_{capture} . For reaction 4 and the reverse reaction IO +
17 HNO₃ involving neutral species, k_{capture} was set to a typical capture rate coefficient of 2.5×10^{-10}
18 $(T/300 \text{ K})^{1/6} \text{ cm}^3 \text{ molecule}^{-1} \text{ s}^{-1}$, where the small positive temperature dependence is
19 characteristic of a long-range potential governed by dispersion and dipole-dipole forces
20 (Georgievskii and Klippenstein, 2005).

21 The probability of collisional transfer between grains was estimated using the exponential down
22 model, where the average energy for downward transitions was set to $\langle \Delta E \rangle_{\text{down}} = 300 \text{ cm}^{-1}$ for
23 N₂ as the third body (Gilbert and Smith, 1990). MESMER determines the temperature- and

1 pressure-dependent rate coefficient from the full microcanonical description of the system time
2 evolution by performing an eigenvector/eigenvalue analysis (Bartis and Widom, 1974). The
3 resulting rate coefficient over the temperature range 260 - 300 K at a pressure of 1000 hPa is
4 $k_4(T) = 2.7 \times 10^{-12} (300 \text{ K} / T)^{2.66} \text{ cm}^3 \text{ molecule}^{-1} \text{ s}^{-1}$. Because the intermediate complexes are
5 not strongly bound, and the transition state and products are below the entrance channel, the only
6 products formed in reaction R4 under atmospheric conditions are IO + HNO₃. The uncertainty in
7 k_4 arises principally from the estimated capture rate coefficient (see above), and absence of a
8 barrier above the entrance channel, and the fact that the intermediate complexes and barrier are
9 well below the entrance channel within their uncertainties, means that the uncertainty in k_4
10 principally arises from the estimated capture rate coefficient the height of the barrier below the
11 entrance channel. As discussed above, the spin-orbit correction of the transition state is likely to
12 be larger than the value of -5.9 kJ mol⁻¹ corresponding to HOI, so k_4 is possibly a lower limit. For
13 instance, if the barrier height is decreased by 3 kJ mol⁻¹, k_4 increases by a factor and so is likely to
14 be no more than a factor of 1.92. If the barrier is lower by 8.5 kJ mol⁻¹ (corresponding to the
15 transition state having the same spin-orbit correction as IO), then k_4 would increase by a factor of
16 5.1. Nevertheless, noting that the capture rate coefficient could be lower – perhaps by a factor of
17 2 - than the estimate used here, we prefer to use the value for k_4 calculated with the potential
18 surface in Figure 3. Of course, if k_4 is larger, then the atmospheric impacts of reaction 4
19 discussed in Section 4 will be even more pronounced.

20 Note that NO₃ also reacts with CH₂I₂ with a rate constant $\sim 2\text{-}4 \times 10^{-13} \text{ cm}^3 \text{ molecule}^{-1} \text{ s}^{-1}$, which
21 can have a significant effect on nighttime CH₂I₂ concentration (Carpenter et al., 2015). However
22 the products of this reaction are still uncertain (Nakano et al., 2006; Carpenter et al., 2015) and
23 its rate is considerably slower than that of R4.

1 In summary, the only likely gas-phase reactions that I₂ and HOI undergo in the nighttime
2 troposphere are R1 and R4, respectively. These are included in the model reaction scheme to
3 examine their impacts on the evolution of iodine species in the atmosphere.

4

5 **4. Atmospheric modelling**

6 We use two atmospheric chemical transport models to study *i*) the impact of this new chemistry
7 on the nighttime chemistry and partitioning of iodine species, and *ii*) the resulting geographical
8 distribution of nocturnal iodine and impact on NO₃ within the global marine boundary layer.

9 The first model, Tropospheric HAlogen chemistry MOdel (THAMO), is used for a detailed
10 kinetics study of the impact of the different reactions shown in Table 1 as well as to assess which
11 uptake rates best reproduce observations from a field study at the CVAO (Carpenter et al., 2011).
12 THAMO has been used in the past to study iodine chemistry at the CVAO and further details
13 including the full chemical scheme can be found elsewhere (Read et al., 2008; Saiz-Lopez et al.,
14 2008; Mahajan et al., 2009; Mahajan et al., 2010a; Mahajan et al., 2010b; Lawler et al., 2014).
15 Briefly, THAMO is a 1-D chemistry transport model with 200 stacked boxes at a vertical
16 resolution of 5m (total height 1 km). The model treats iodine, bromine, O₃, NO_x and HO_x
17 chemistry, and is constrained with typical measured values of other chemical species in the
18 MBL: [CO]=110 nmol mol⁻¹; [DMS]=30 pmol/mol; [CH₄]=1820 nmol mol⁻¹; [ethane]=925
19 pmol/mol; [CH₃CHO]=970 pmol/mol; [HCHO]=500 pmol/mol; [isoprene]=10 pmol/mol;
20 [propane]=60 pmol/mol; [propene]=20 pmol/mol. The average background aerosol surface area
21 (ASA) used is 1x10⁻⁶ cm² cm⁻³ (Read et al., 2008; Lee et al., 2009; Read et al., 2009; Lee et al.,

1 2010). The model is initialized at midnight and the evolution of iodine species, O₃, NO_x and HO_x
2 is followed until the model reaches steady state.

3 The second model is the global 3D chemistry-climate model CAM-Chem (Community
4 Atmospheric Model with chemistry, version 4.0), which is used to study the impact of reactions
5 1 and 4 on a global scale. The model includes a comprehensive chemistry scheme to simulate the
6 evolution of trace gases and aerosols in the troposphere and the stratosphere (Lamarque et al.,
7 2012). The model runs with the iodine and bromine chemistry schemes from previous studies
8 (Fernandez et al., 2014; Saiz-Lopez et al., 2014; Saiz-Lopez et al., 2015), including the
9 photochemical breakdown of bromo- and iodo-carbons emitted from the oceans (Ordóñez et al.,
10 2012) and abiotic oceanic sources of HOI and I₂ (Prados-Roman et al., 2015a). CAM-Chem has
11 been configured in this work with a horizontal resolution of 1.9° latitude by 2.5° longitude and 26
12 vertical levels, from the surface to ~40km altitude. All model runs in this study were performed
13 in the specified dynamics mode (Lamarque et al., 2012) using offline meteorological fields
14 instead of an online calculation, to allow direct comparisons between different simulations. This
15 offline meteorology consists of a high frequency meteorological input from a previous free
16 running climatic simulation.

17 It should be noted that during nighttime the uptake on aerosols of emitted species such as I₂ and
18 HOI, and the uptake of reservoir species such as IONO₂, can play a major role in the cycling of
19 iodine. Observations at CVAO show that I₂ peaked at about 1 pmol/mol during the night and that
20 ICl was not detected above the 1 pmol/mol detection limit of the instrument (Lawler et al.,
21 2014). In order to match these observations, we need to reduce the uptake and heterogeneous
22 recycling of iodine species. The uptake rates of chemical species on the background seasalt
23 aerosols are determined by their uptake coefficients (γ). The database of mass accommodation

1 and/or uptake coefficients is rather sparse and essentially limited to I₂, HI, HOI, ICl, IBr on pure
2 water/ice and on sulphuric acid particles (Sander et al., 2006). Other iodine species which are
3 likely to undergo uptake onto aerosol are OIO, HIO₃, INO₂, IONO₂, I₂O₂ (Saiz-Lopez et al.,
4 2012a; Sommariva et al., 2012). Uptake of HOI is very uncertain, with $\gamma(\text{HOI})$ ranging from $2 \times$
5 10^{-3} to 0.3 depending on the surface composition and state (Holmes et al., 2001). Sommariva et
6 al. (2012) assumed $\gamma(\text{HOI})$ to be 0.6, similar to the value for HOBr measured by Wachsmuth et
7 al. (2002). In the case of IONO₂, the uptake coefficient has not been measured, with most models
8 using values of 0.1 (von Glasow et al., 2002; Saiz-Lopez et al., 2008; Mahajan et al., 2009; Leigh
9 et al., 2010; Mahajan et al., 2010a; Mahajan et al., 2010b; Sommariva et al., 2012; Lawler et al.,
10 2014). The modelled levels of I₂ and ICl change with different values of uptake coefficients. To
11 match the CVAO I₂ and ICl observations (Lawler et al., 2014), we have used $\gamma = 0.01$ for HOI
12 and IONO₂, which is within the uncertainty in the literature, and assumed that 80% is recycled as
13 I₂. Further measurements of these dihalogen species are needed to better constrain their
14 heterogeneous recycling on seasalt aerosols.

15

16 **5. Results and discussion**

17 Of the possible nocturnal iodine activation reactions involving the inorganic iodine source gases
18 I₂ and HOI, only reactions R1 and R4 appear to be likely candidates (see Section 3). We
19 therefore designed two modelling scenarios: Scenario 1 (S1), without nighttime reactions of I₂ or
20 HOI with NO₃; and Scenario 2 (S2), including reactions R1 and R4 for the degradation of HOI
21 and I₂ by NO₃. In the one-dimensional model THAMO, the I₂ and HOI are injected into the
22 atmosphere from the ocean surface using the flux parameterizations derived from laboratory

1 experiments (Carpenter et al., 2013; MacDonald et al., 2014). Figure 4 shows the resulting
2 diurnal evolution of the HOI and I₂ mixing ratios in the two scenarios, after two days of
3 simulation time. The I₂ mixing ratio peaks during the night in both the scenarios due to quick
4 loss by photolysis during the daytime. By contrast, HOI is present during daytime due to its
5 production through the reaction of IO with HO₂, and peaks just before sunset. In the first
6 scenario, without the inclusion of reactions R1 and R4, Figure 4 (right-hand side panels) shows
7 that ~~HOI and I₂ both~~ build up during the night, reaching a concentration peak just before dawn.
8 This is especially noticeable ~~for I₂~~ as the daytime concentrations are much lower than during the
9 night. On the other hand, HOI concentrations decrease during night until dawn, when they drop
10 to zero. For both species, inclusion of reactions with NO₃ causes a decrease in their respective
11 nocturnal concentrations (Fig. 4, left-hand side panels). The inclusion of reactions R1 and R4
12 also leads to a modelled I₂ concentration which is in better agreement with the observations of
13 the molecule made at CVAO (Lawler et al., 2014), reaching peak values of about 1 pmol/mol, as
14 compared to about 3 pmol/mol for the scenario without nighttime reactions. An additional
15 consequence of including reactions R1 and R4 is the significant increase of the sea-air fluxes of
16 HOI and I₂ at night due to their atmospheric removal by NO₃ (Fig. 4, bottom panel).

17 Figure 5 shows the diurnal evolution of IO, NO₃ and IONO₂ in both model scenarios after two
18 days of simulation time. Although the daytime peak values of IO are well reproduced in both
19 scenarios, reaching about 1.5 pmol/mol around noon similar to the ground-based observations
20 (Read et al., 2008), the inclusion of reactions R1 and R4 leads to the removal of the dawn spike
21 in IO, which is predicted by current iodine models but was not observed at CVAO (Read et al.,
22 2008; Mahajan et al., 2010a). The IO dawn spike predicted by models is due to a buildup of the
23 emitted I₂ and HOI (which is converted into ~~I₂~~/IBr/ICl through heterogeneous recycling) over the

1 night, followed by rapid photolysis after first sunlight. However, due to the considerable removal
2 of HOI and I₂ through the night due to reaction with ambient NO₃, this spike does not appear in
3 the second scenario, leading to a modification of the diurnal profile of IO that better matches
4 with observations.

5 Reactions R1 and R4 also reduce the NO₃ mixing ratio (Fig. 5, middle panels). In scenario 1, the
6 NO₃ is modelled to peak at about 14 pmol/mol just before dawn. However, the inclusion of
7 reactions R1 and R4 leads to near complete depletion of NO₃ close to the surface, with the peak
8 level at the surface reaching only 2 pmol/mol, since reactions R1 and R4 become the main
9 atmospheric loss processes for NO₃ in the lower MBL. These reactions lead however to the
10 buildup of IONO₂ during the night (Fig. 5, bottom panels). In the absence of reactions R1 and
11 R4, significant levels of IONO₂ are seen only at dawn and dusk since no other reactions produce
12 IONO₂ at night, and during the day IONO₂ is removed by photolysis. However, with continuous
13 conversion of I₂ and HOI to IONO₂ by reactions R1 and R4 in scenario 2, IONO₂ is modelled to
14 reach up to 3 pmol/mol in the nocturnal MBL.

15 Given the associated uncertainty in the theoretical estimate of the k_4 , we used THAMO to assess
16 the sensitivity of surface NO₃ to k_4 . Figure 6 shows that NO₃ [peak nighttime concentration](#) is in
17 fact highly coupled to k_4 , with the expected uncertainty in k_4 of one order of magnitude (see
18 above) giving rise to a factor of two change in NO₃. A laboratory measurement of k_4 should
19 therefore be undertaken in the future.

20 We now implement the nighttime reactions in the 3D global model (CAM-Chem) to assess the
21 resulting geographical distributions and impacts of these reactions. We have also run two
22 different scenarios in CAM-Chem, the first without R1 and R4 in the chemical scheme, and the

1 second including the new nighttime iodine chemistry. Figure 7 shows how the inclusion of R1
2 and R4 reduces globally the nighttime concentrations of I_2 and HOI. The plots correspond to the
3 nighttime averaged (from 00LT to 01LT ([Local Time](#))) differences between the model scenarios.
4 Considerable reductions of up to 0.5 and 10 pmol/mol (i.e. up to 100% removal) are observed for
5 I_2 and HOI, respectively, particularly over coastal polluted regions where continental pollution
6 outflow leads to higher levels of NO_3 in the nighttime MBL. Major shipping routes also show
7 strong nocturnal iodine activity due to the characteristically high NO_x , and resulting NO_3 ,
8 associated with shipping emissions.

9 Figure 8 shows the effect of this nocturnal chemistry on the concentrations of $IONO_2$ and NO_3 .
10 As in the previous figure, the plots correspond to the nighttime averaged difference between the
11 second and the first scenarios. The maps show an increase of $IONO_2$ of up to 15 pmol/mol
12 (~600%) over polluted coastal areas, due to efficient conversion of NO_3 into $IONO_2$. The bottom
13 panel of Figure 7 shows the expected decrease of NO_3 levels associated with the inclusion of
14 reactions R1 and R4, with decreases of up to ~4 pmol/mol (up to 60%) over marine polluted
15 regions. We model global percentage reductions in the NO_3 concentrations of 7.1% (60S-60N),
16 with nitrate removal of up to 80% in non-polluted remote oceanic regions with low NO_3 levels.
17 This in turn can affect the modelled oxidation of DMS by NO_3 . We estimate that the reduction in
18 NO_3 , due to the inclusion of R1 and R4, results in a model increase in DMS levels of up to 7
19 pmol/mol (about 20%) in marine regions affected by continental pollution outflow (Fig. 9). We
20 therefore suggest that the inclusion of the new nighttime iodine chemistry can have a large, so far
21 unrecognized, impact on the nocturnal oxidizing capacity of the marine atmosphere.

22 The hourly evolution of the main species involved in this study is shown in Figures 10 and 11,
23 which include the levels of HOI, I_2 , $IONO_2$ and NO_3 in the MBL over regions where nocturnal

1 iodine is modelled to be particularly active. The first region is located within the Mediterranean
2 Sea, an area that shows large differences during the summer months when high ozone levels
3 drive large emissions of HOI and I₂ from the sea, and the high levels of NO₃ at nighttime make
4 this chemistry especially important. The hourly average in August is shown in Figure 10 for
5 HOI, IONO₂ and I₂. HOI and IONO₂ (Fig 10) are the species whose concentration differ most
6 between scenarios as HOI is removed and IONO₂ produced by R4 (and, to a lesser extent, R1).
7 Over a Pacific Ocean region at the south of the Baja California Peninsula, the modelled
8 differences between the two scenarios are even higher than over the Mediterranean Sea (Figure
9 11). Large differences in MBL NO₃, up to 28%, are modelled during the night caused by
10 pollution outflow from the west coasts of Mexico and USA.

11

12 **6. Summary and conclusions**

13 The viability of the reaction of HOI with NO₂, HNO₃ and NO₃ has been studied by theoretical
14 calculations. The results indicate that only the reaction of HOI with NO₃, to yield IO + HNO₃, is
15 possible under tropospheric conditions. The inclusion of this reaction, along with that of I₂ +
16 NO₃, has a number of significant implications: *i*) nocturnal iodine radical chemistry is activated;
17 *ii*) this causes enhanced nighttime oceanic emissions of HOI and I₂; *iii*) nighttime iodine species
18 are partitioned into high levels of IONO₂; *iv*) the IO spike, modelled by current iodine models
19 but not shown by observations, is removed; and, *v*) a reduction of the levels of nitrate radical in
20 the MBL, with the associated less efficient oxidation of DMS, which has important implications
21 for our understanding of the nocturnal oxidizing capacity of the marine atmosphere.

22

1

2 **Acknowledgments**

3 This work was supported by the Spanish National Research Council (CSIC). The National
4 Center for Atmospheric Research (NCAR) is funded by the National Science Foundation NSF.
5 The Climate Simulation Laboratory at NCAR's Computational and Information Systems
6 Laboratory (CISL) provided the computing resources (ark:/85065/d7wd3xhc). As part of the
7 CESM project, CAM-Chem is supported by the NSF and the Office of Science (BER) of the US
8 Department of Energy. This work was also sponsored by the NASA Atmospheric Composition
9 Modeling and Analysis Program Activities (ACMAP, number NNX11AH90G).

10

11 **References**

- 12 Allan, B. J., McFiggans, G., Plane, J. M. C., Coe, H., and McFadyen, G. G.: The nitrate radical
13 in the remote marine boundary layer, *Journal of Geophysical Research: Atmospheres*, 105,
14 24191-24204, 10.1029/2000jd900314, 2000.
- 15 Allan, J. D., Williams, P. I., Najera, J., Whitehead, J. D., Flynn, M. J., Taylor, J. W., Liu, D.,
16 Darbyshire, E., Carpenter, L. J., Chance, R., Andrews, S. J., Hackenberg, S. C., and McFiggans,
17 G.: Iodine observed in new particle formation events in the Arctic atmosphere during
18 ACCACIA, *Atmos. Chem. Phys.*, 15, 5599-5609, 10.5194/acp-15-5599-2015, 2015.
- 19 Bartis, J. T., and Widom, B.: Stochastic models of the interconversion of three or more chemical
20 species, *J. Chem. Phys.*, 60, 3474-3482, doi: 10.1063/1.1681562, 1974.

1 Butler, J. H., King, D. B., Lobert, J. M., Montzka, S. A., Yvon-Lewis, S. A., Hall, B. D.,
2 Warwick, N. J., Mondeel, D. J., Aydin, M., and Elkins, J. W.: Oceanic distributions and
3 emissions of short-lived halocarbons, *Global Biogeochem. Cycles*, 21, GB1023,
4 10.1029/2006gb002732, 2007.

5 Carpenter, L. J.: Iodine In the marine Boundary Layer, *Chem. Rev.*, 103 (12), 4953-4962, 2003.

6 Carpenter, L. J., Fleming, Z. L., Read, K. A., Lee, J. D., Moller, S. J., Hopkins, J. R., Purvis, R.
7 M., Lewis, A. C., Müller, K., Heinold, B., Herrmann, H., Fomba, K. W., Pinxteren, D., Müller,
8 C., Tegen, I., Wiedensohler, A., Müller, T., Niedermeier, N., Achterberg, E. P., Patey, M. D.,
9 Kozlova, E. A., Heimann, M., Heard, D. E., Plane, J. M. C., Mahajan, A., Oetjen, H., Ingham, T.,
10 Stone, D., Whalley, L. K., Evans, M. J., Pilling, M. J., Leigh, R. J., Monks, P. S., Karunaharan,
11 A., Vaughan, S., Arnold, S. R., Tschritter, J., Pöhler, D., Frieß, U., Holla, R., Mendes, L. M.,
12 Lopez, H., Faria, B., Manning, A. J., and Wallace, D. W. R.: Seasonal characteristics of tropical
13 marine boundary layer air measured at the Cape Verde Atmospheric Observatory, *J. Atmos.*
14 *Chem.*, 67, 87-140, 10.1007/s10874-011-9206-1, 2011.

15 Carpenter, L. J., MacDonald, S. M., Shaw, M. D., Kumar, R., Saunders, R. W., Parthipan, R.,
16 Wilson, J., and Plane, J. M. C.: Atmospheric iodine levels influenced by sea surface emissions of
17 inorganic iodine, *Nature Geosci*, 6, 108-111, 10.1038/ngeo1687, 2013.

18 Carpenter, L. J., Andrews, S. J., Lidster, R. T., Saiz-Lopez, A., Fernandez-Sanchez, M., Bloss,
19 W. J., Ouyang, B., and Jones, R. L.: A nocturnal atmospheric loss of
20 CH_2I_2 in the remote marine boundary layer, *J. Atmos. Chem.*,
21 10.1007/s10874-015-9320-6, 2015.

1 Fernandez, R. P., Salawitch, R. J., Kinnison, D. E., Lamarque, J. F., and Saiz-Lopez, A.:
2 Bromine partitioning in the tropical tropopause layer: implications for stratospheric injection,
3 *Atmos. Chem. Phys.*, 14, 13391-13410, 10.5194/acp-14-13391-2014, 2014.

4 Frisch, M., Trucks, G., Schlegel, H., Scuseria, G., Robb, M., Cheeseman, J., Scalmani, G.,
5 Barone, V., Mennucci, B., and Petersson, G.: *Gaussian 09*, Revision A. 1. Wallingford, CT:
6 Gaussian, in, Inc, 2009.

7 Georgievskii, Y., and Klippenstein, S. J.: Long-range transition state theory, *J. Chem. Phys.*, 122,
8 194103, doi: 10.1063/1.1899603, 2005.

9 Gilbert, R. G., and Smith, S. C.: *Theory of Unimolecular and Recombination Reactions*,
10 Blackwell, Oxford, 1990.

11 Glukhovtsev, M. N., Pross, A., McGrath, M. P., and Radom, L.: Extension of Gaussian-2 (G2)
12 theory to bromine- and iodine-containing molecules: Use of effective core potentials, *J. Chem.*
13 *Phys.*, 103, 1878-1885, 1995.

14 Gomez Martin, J. C., Galvez, O., Baeza-Romero, M. T., Ingham, T., Plane, J. M. C., and Blitz,
15 M. A.: On the mechanism of iodine oxide particle formation, *Phys. Chem. Chem. Phys.*, 15,
16 15612-15622, 10.1039/c3cp51217g, 2013.

17 Gómez Martín, J. C., Mahajan, A. S., Hay, T. D., Prados-Román, C., Ordóñez, C., MacDonald,
18 S. M., Plane, J. M. C., Sorribas, M., Gil, M., Paredes Mora, J. F., Agama Reyes, M. V., Oram, D.
19 E., Leedham, E., and Saiz-Lopez, A.: Iodine chemistry in the eastern Pacific marine boundary
20 layer, *Journal of Geophysical Research: Atmospheres*, 118, 887-904, 10.1002/jgrd.50132, 2013.

- 1 Großmann, K., Frieß, U., Peters, E., Wittrock, F., Lampel, J., Yilmaz, S., Tschritter, J.,
2 Sommariva, R., von Glasow, R., Quack, B., Krüger, K., Pfeilsticker, K., and Platt, U.: Iodine
3 monoxide in the Western Pacific marine boundary layer, *Atmos. Chem. Phys.*, 13, 3363-3378,
4 10.5194/acp-13-3363-2013, 2013.
- 5 Hoffmann, T., O'Dowd, C. D., and Seinfeld, J. H.: Iodine oxide homogeneous nucleation: An
6 explanation for coastal new particle production, *Geophys. Res. Lett.*, 28, 1949-1952, 2001.
- 7 Holmes, N. S., Adams, J. W., and Crowley, J. N.: Uptake and reaction of HOI and IONO₂ on
8 frozen and dry NaCl/NaBr surfaces and H₂SO₄, *Phys. Chem. Chem. Phys.*, 3, 1679-1687,
9 10.1039/b100247n, 2001.
- 10 Jones, C. E., Hornsby, K. E., Sommariva, R., Dunk, R. M., von Glasow, R., McFiggans, G., and
11 Carpenter, L. J.: Quantifying the contribution of marine organic gases to atmospheric iodine,
12 *Geophys. Res. Lett.*, 37, L18804, 2010.
- 13 Kaltsoyannis, N., and Plane, J. M. C.: Quantum chemical calculations on a selection of iodine-
14 containing species (IO, OIO, INO₃, (IO)₂, I₂O₃, I₂O₄ and I₂O₅) of importance in the atmosphere.,
15 *Phys. Chem. Chem. Phys.*, 10, 1723-1733, 2008.
- 16 Khanniche, S., Louis, F., Cantrel, L., and Černušák, I.: A Density Functional Theory and ab
17 Initio Investigation of the Oxidation Reaction of CO by IO Radicals, *J. Phys. Chem. A*, 120,
18 1737–1749, 2016.
- 19 Lamarque, J. F., Emmons, L. K., Hess, P. G., Kinnison, D. E., Tilmes, S., Vitt, F., Heald, C. L.,
20 Holland, E. A., Lauritzen, P. H., Neu, J., Orlando, J. J., Rasch, P. J., and Tyndall, G. K.: CAM-

1 chem: description and evaluation of interactive atmospheric chemistry in the Community Earth
2 System Model, *Geosci. Model Dev.*, 5, 369-411, 10.5194/gmd-5-369-2012, 2012.

3 Lawler, M. J., Mahajan, A. S., Saiz-Lopez, A., and Saltzman, E. S.: Observations of I₂ at a
4 remote marine site, *Atmos. Chem. Phys.*, 14, 2669-2678, 10.5194/acp-14-2669-2014, 2014.

5 Lee, J. D., Moller, S. J., Read, K. A., Lewis, A. C., Mendes, L., and Carpenter, L. J.: Year-round
6 measurements of nitrogen oxides and ozone in the tropical North Atlantic marine boundary layer,
7 *Journal of Geophysical Research: Atmospheres*, 114, n/a-n/a, 10.1029/2009jd011878, 2009.

8 Lee, J. D., McFiggans, G., Allan, J. D., Baker, A. R., Ball, S. M., Benton, A. K., Carpenter, L. J.,
9 Commane, R., Finley, B. D., Evans, M., Fuentes, E., Furneaux, K., Goddard, A., Good, N.,
10 Hamilton, J. F., Heard, D. E., Herrmann, H., Hollingsworth, A., Hopkins, J. R., Ingham, T.,
11 Irwin, M., Jones, C. E., Jones, R. L., Keene, W. C., Lawler, M. J., Lehmann, S., Lewis, A. C.,
12 Long, M. S., Mahajan, A., Methven, J., Moller, S. J., Müller, K., Müller, T., Niedermeier, N.,
13 O'Doherty, S., Oetjen, H., Plane, J. M. C., Pszenny, A. A. P., Read, K. A., Saiz-Lopez, A.,
14 Saltzman, E. S., Sander, R., von Glasow, R., Whalley, L., Wiedensohler, A., and Young, D.:
15 Reactive Halogens in the Marine Boundary Layer (RHAMBLE): the tropical North Atlantic
16 experiments, *Atmos. Chem. Phys.*, 10, 1031-1055, 10.5194/acp-10-1031-2010, 2010.

17 Leigh, R. J., Ball, S. M., Whitehead, J., Leblanc, C., Shillings, A. J. L., Mahajan, A. S., Oetjen,
18 H., Dorsey, J. R., Gallagher, M., Jones, R. L., Plane, J. M. C., Potin, P., and McFiggans, G.:
19 Measurements and modelling of molecular iodine emissions, transport and photodestruction in
20 the coastal region around Roscoff, *Atmos. Chem. Phys.*, 10, 11823-11838, 2010.

1 MacDonald, S. M., Gómez Martín, J. C., Chance, R., Warriner, S., Saiz-Lopez, A., Carpenter, L.
2 J., and Plane, J. M. C.: A laboratory characterisation of inorganic iodine emissions from the sea
3 surface: dependence on oceanic variables and parameterisation for global modelling, *Atmos.*
4 *Chem. Phys.*, 14, 5841-5852, 10.5194/acp-14-5841-2014, 2014.

5 Mahajan, A. S., Oetjen, H., Saiz-Lopez, A., Lee, J. D., McFiggans, G. B., and Plane, J. M. C.:
6 Reactive iodine species in a semi-polluted environment, *Geophys. Res. Lett.*, 36, L16803,
7 doi:16810.11029/12009GL038018, 2009.

8 Mahajan, A. S., Plane, J. M. C., Oetjen, H., Mendes, L., Saunders, R. W., Saiz-Lopez, A., Jones,
9 C. E., Carpenter, L. J., and McFiggans, G. B.: Measurement and modelling of tropospheric
10 reactive halogen species over the tropical Atlantic Ocean, *Atmos. Chem. Phys.*, 10, 4611-4624,
11 2010a.

12 Mahajan, A. S., Shaw, M., Oetjen, H., Hornsby, K. E., Carpenter, L. J., Kaleschke, L., Tian-
13 Kunze, X., Lee, J. D., Moller, S. J., Edwards, P., Commane, R., Ingham, T., Heard, D. E., and
14 Plane, J. M. C.: Evidence of reactive iodine chemistry in the Arctic boundary layer, *J. Geophys.*
15 *Res.*, [Atmos.], 115, D20303, doi:10.1029/2009JD013665, 2010b.

16 Mahajan, A. S., Gómez Martín, J. C., Hay, T. D., Royer, S. J., Yvon-Lewis, S., Liu, Y., Hu, L.,
17 Prados-Roman, C., Ordóñez, C., Plane, J. M. C., and Saiz-Lopez, A.: Latitudinal distribution of
18 reactive iodine in the Eastern Pacific and its link to open ocean sources, *Atmos. Chem. Phys.*, 12,
19 11609-11617, 10.5194/acp-12-11609-2012, 2012.

20 McFiggans, G., Coe, H., Burgess, R., Allan, J., Cubison, M., Alfarra, M. R., Saunders, R., Saiz-
21 Lopez, A., Plane, J. M. C., Wevill, D. J., Carpenter, L. J., Rickard, A. R., and Monks, P. S.:

- 1 Direct evidence for coastal iodine particles from *Laminaria* macroalgae - linkage to emissions of
2 molecular iodine, *Atmos. Chem. Phys.*, 4, 701-713, 2004.
- 3 Mečiarová, K., Šulka, M., Canneaux, S., Louis, F., and Černušáka, I.: A theoretical study of the
4 kinetics of the forward and reverse reactions $\text{HI} + \text{CH}_3 = \text{I} + \text{CH}_4$, *Chem. Phys. Lett.*, 517, 149-
5 154, 2011.
- 6 Nakano, Y., Ukeguchi, H., and Ishiwata, T.: Rate constant of the reaction of NO_3 with CH_2I_2
7 measured with use of cavity ring-down spectroscopy, *Chem. Phys. Lett.*, 430, 235-239, doi:
8 10.1016/j.cplett.2006.09.002, 2006.
- 9 O'Dowd, C. D., Jimenez, J. L., Bahreini, R., Flagan, R. C., Seinfeld, J. H., Hameri, K., Pirjola,
10 L., Kulmala, M., Jennings, S. G., and Hoffmann, T.: Marine aerosol formation from biogenic
11 iodine emissions, *Nature*, 417, 632-636, 2002.
- 12 Ordóñez, C., Lamarque, J. F., Tilmes, S., Kinnison, D. E., Atlas, E. L., Blake, D. R., Sousa
13 Santos, G., Brasseur, G., and Saiz-Lopez, A.: Bromine and iodine chemistry in a global
14 chemistry-climate model: description and evaluation of very short-lived oceanic sources, *Atmos.*
15 *Chem. Phys.*, 12, 1423-1447, 10.5194/acp-12-1423-2012, 2012.
- 16 Plane, J. M. C., Joseph, D. M., Allan, B. J., Ashworth, S. H., and Francisco, J. S.: An
17 Experimental and Theoretical Study of the Reactions $\text{OIO} + \text{NO}$ and $\text{OIO} + \text{OH}$, *J. Phys. Chem.*
18 *A*, 110, 93-100, 2006.
- 19 Prados-Roman, C., Cuevas, C. A., Fernandez, R. P., Kinnison, D. E., Lamarque, J. F., and Saiz-
20 Lopez, A.: A negative feedback between anthropogenic ozone pollution and enhanced ocean
21 emissions of iodine, *Atmos. Chem. Phys.*, 15, 2215-2224, 10.5194/acp-15-2215-2015, 2015a.

1 Prados-Roman, C., Cuevas, C. A., Hay, T., Fernandez, R. P., Mahajan, A. S., Royer, S. J., Galí,
2 M., Simó, R., Dachs, J., Großmann, K., Kinnison, D. E., Lamarque, J. F., and Saiz-Lopez, A.:
3 Iodine oxide in the global marine boundary layer, *Atmos. Chem. Phys.*, 15, 583-593,
4 10.5194/acp-15-583-2015, 2015b.

5 Read, K. A., Mahajan, A. S., Carpenter, L. J., Evans, M. J., Faria, B. V. E., Heard, D. E.,
6 Hopkins, J. R., Lee, J. D., Moller, S. J., Lewis, A. C., Mendes, L., McQuaid, J. B., Oetjen, H.,
7 Saiz-Lopez, A., Pilling, M. J., and Plane, J. M. C.: Extensive halogen-mediated ozone
8 destruction over the tropical Atlantic Ocean, *Nature*, 453, 1232-1235, 2008.

9 Read, K. A., Lee, J. D., Lewis, A. C., Moller, S. J., Mendes, L., and Carpenter, L. J.: Intra-annual
10 cycles of NMVOC in the tropical marine boundary layer and their use for interpreting seasonal
11 variability in CO, *Journal of Geophysical Research: Atmospheres*, 114, n/a-n/a,
12 10.1029/2009jd011879, 2009.

13 Roberston, S. H., Glowacki, D. R., Liang, C. H., Morley, C., Shannon, R., Blitz, M., and Pilling,
14 M. J.: MESMER (Master Equation Solver for Multi-Energy Well Reactions), 2008–2012: An
15 object oriented C++ program for carrying out ME calculations and eigenvalue-eigenvector
16 analysis on arbitrary multiple well systems, edited. [Available at
17 <http://sourceforge.net/projects/mesmer>.], in, 4.1 ed., 2014.

18 Roscoe, H. K., Jones, A. E., Brough, N., Weller, R., Saiz-Lopez, A., Mahajan, A. S.,
19 Schoenhardt, A., Burrows, J. P., and Fleming, Z. L.: Particles and iodine compounds in coastal
20 Antarctica, *Journal of Geophysical Research: Atmospheres*, 120, 7144-7156,
21 10.1002/2015jd023301, 2015.

1 Saiz-Lopez, A., and Plane, J. M. C.: Novel iodine chemistry in the marine boundary layer,
2 *Geophys. Res. Lett.*, 31, L04112, 2004.

3 Saiz-Lopez, A., Plane, J. M. C., Mahajan, A. S., Anderson, P. S., Bauguitte, S. J.-B., Jones, A.
4 E., Roscoe, H. K., Salmon, R. A., Bloss, W. J., Lee, J. D., and Heard, D. E.: On the vertical
5 distribution of boundary layer halogens over coastal Antarctica: implications for O₃, HO_x, NO_x
6 and the Hg lifetime, *Atmos. Chem. Phys.*, 8, 887-900, 2008.

7 Saiz-Lopez, A., Lamarque, J.-F., Kinnison, D., Tilmes, S., Ordóñez, C., Orlando, J. J., Conley,
8 A. J., Plane, J. M. C., Mahajan, A., Sousa Santos, G., Atlas, E., Blake, D. R., Sander, S. P.,
9 Schauflier, S. M., Thompson, A. M., and Brasseur, G.: Estimating the climate significance of
10 halogen-driven ozone loss in the tropical marine troposphere, *Atmos. Chem. Phys.*, 12, 3939-
11 3949, 2012a.

12 Saiz-Lopez, A., Plane, J. M. C., Baker, A. R., Carpenter, L. J., Von Glasow, R., Gómez Martín,
13 J. C., McFiggans, G., and Saunders, R. W.: Atmospheric Chemistry of Iodine, *Chem. Rev.*
14 (Washington, DC, U. S.), 112, 1773-1804, 10.1021/cr200029u, 2012b.

15 Saiz-Lopez, A., Fernandez, R. P., Ordóñez, C., Kinnison, D. E., Gómez Martín, J. C., Lamarque,
16 J. F., and Tilmes, S.: Iodine chemistry in the troposphere and its effect on ozone, *Atmos. Chem.*
17 *Phys.*, 14, 13119-13143, 10.5194/acp-14-13119-2014, 2014.

18 Saiz-Lopez, A., Baidar, S., Cuevas, C. A., Koenig, T. K., Fernandez, R. P., Dix, B., Kinnison, D.
19 E., Lamarque, J. F., Rodriguez-Lloveras, X., Campos, T. L., and Volkamer, R.: Injection of
20 iodine to the stratosphere, *Geophys. Res. Lett.*, n/a-n/a, 10.1002/2015gl064796, 2015.

1 Sander, S. P., Orkin, V. L., Kurylo, M. J., Golden, D. M., Huie, R. E., Kolb, C. E., Finlayson-
2 Pitts, B. J., Molina, M. J., Friedl, R. R., Ravishankara, A. R., Moortgat, G. K., Keller-Rudek, H.,
3 and Wine, P. H.: Chemical kinetics and photochemical data for use in atmospheric studies, JPL-
4 NASA, 2006.

5 Sherwen, T., Evans, M. J., Carpenter, L. J., Andrews, S. J., Lidster, R. T., Dix, B., Koenig, T. K.,
6 Sinreich, R., Ortega, I., Volkamer, R., Saiz-Lopez, A., Prados-Roman, C., Mahajan, A. S., and
7 Ordóñez, C.: Iodine's impact on tropospheric oxidants: a global model study in GEOS-Chem,
8 *Atmos. Chem. Phys.*, 16, 1161-1186, 10.5194/acp-16-1161-2016, 2016.

9 Simpson, W. R., Brown, S. S., Saiz-Lopez, A., Thornton, J. A., and Glasow, R. v.: Tropospheric
10 Halogen Chemistry: Sources, Cycling, and Impacts, *Chem. Rev.*, 115, 4035-4062,
11 10.1021/cr5006638, 2015.

12 Sommariva, R., Bloss, W. J., and von Glasow, R.: Uncertainties in gas-phase atmospheric iodine
13 chemistry, *Atmos. Environ.*, 57, 219-232, doi: 10.1016/j.atmosenv.2012.04.032, 2012.

14 Šulková, K., Šulka, M., Louis, F., and Neogrady, P.: Atmospheric Reactivity of CH₂ICl with OH
15 Radicals: High-Level OVOS CCSD(T) Calculations for the X-Abstraction Pathways (X = H, Cl,
16 or I), *J. Phys. Chem. A*, 117, 771–782, 2013.

17 Volkamer, R., Baidar, S., Campos, T. L., Coburn, S., DiGangi, J. P., Dix, B., Eloranta, E. W.,
18 Koenig, T. K., Morley, B., Ortega, I., Pierce, B. R., Reeves, M., Sinreich, R., Wang, S., Zondlo,
19 M. A., and Romashkin, P. A.: Aircraft measurements of BrO, IO, glyoxal, NO₂, H₂O, O₂–O₂
20 and aerosol extinction profiles in the tropics: comparison with aircraft-/ship-based in situ and
21 lidar measurements, *Atmos. Meas. Tech.*, 8, 2121-2148, 10.5194/amt-8-2121-2015, 2015.

1 von Glasow, R., Sander, R., Bott, A., and Crutzen, P. J.: Modeling halogen chemistry in the
2 marine boundary layer. 1. Cloud-free MBL, *J. Geophys. Res.*, 107, 4341, 2002.

3 Wachsmuth, M., Gäggeler, H. W., von Glasow, R., and Ammann, M.: Accommodation
4 coefficient of HOBr on deliquescent sodium bromide aerosol particles, *Atmos. Chem. Phys.*, 2,
5 121-131, 10.5194/acp-2-121-2002, 2002.

6 Wang, F., Saiz-Lopez, A., Mahajan, A. S., Gómez Martín, J. C., Armstrong, D., Lemes, M., Hay,
7 T., and Prados-Roman, C.: Enhanced production of oxidised mercury over the tropical Pacific
8 Ocean: a key missing oxidation pathway, *Atmos. Chem. Phys.*, 14, 1323-1335, 10.5194/acp-14-
9 1323-2014, 2014.

10

11

1 **Tables**

2

3 Table 1: Night time reactions of emitted inorganic iodine compounds considered in addition to
 4 the iodine chemistry scheme used by (Saiz-Lopez et al., 2014).

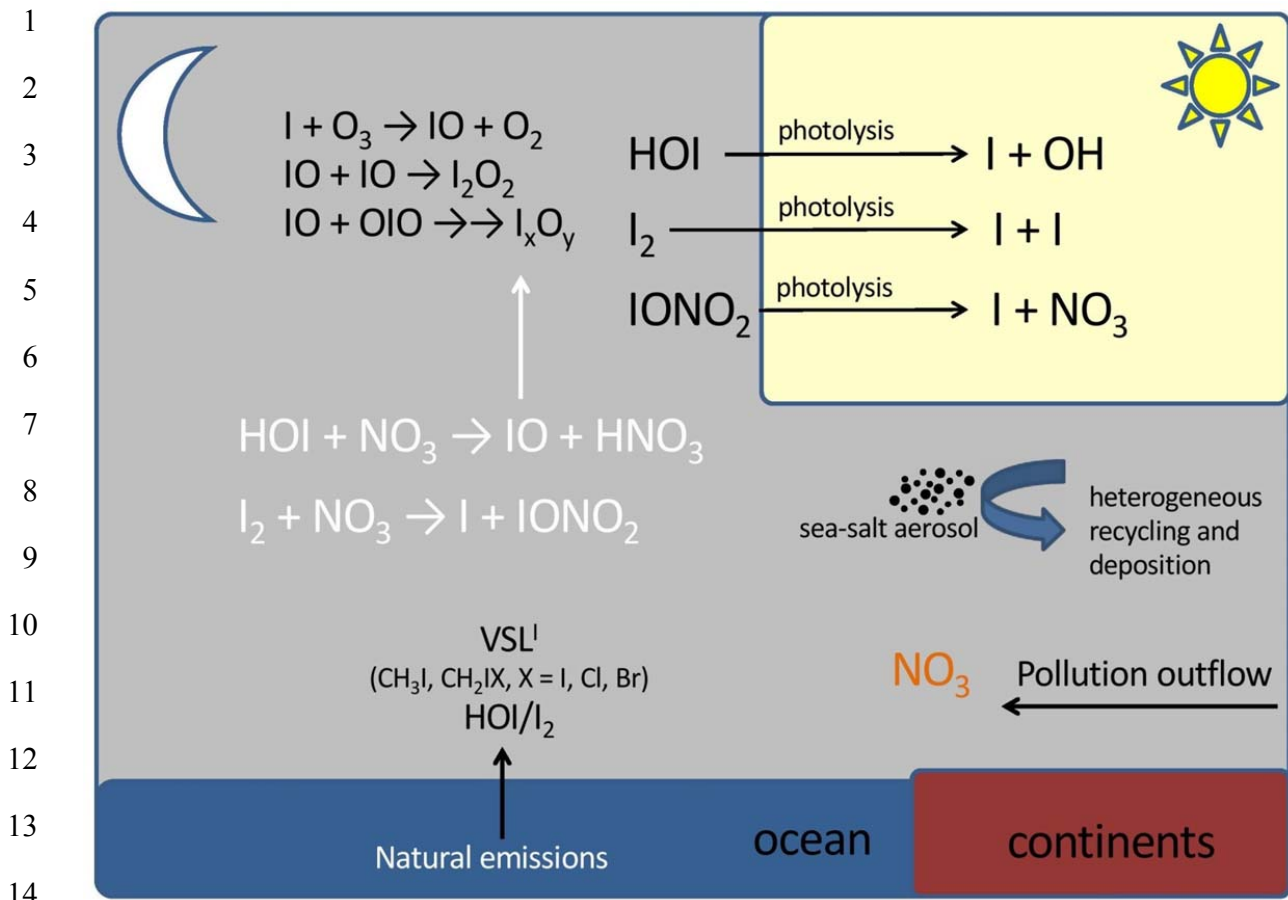
No.	Reaction	Notes
R1.	$I_2 + NO_3 \rightarrow I + IONO_2$	$1.5 \times 10^{-12} \text{ cm}^3 \text{ molecule}^{-1} \text{ s}^{-1}$ [<i>Chambers et al.</i> , 1992]
R2.	$HOI + NO_2 \rightarrow I + HNO_3$	Endothermic by 9 kJ mol^{-1} and the transition state is 73 kJ mol^{-1} above the reactants
R3.	$HOI + HNO_3 \rightarrow IONO_2 + H_2O$	Exothermic by 11 kJ mol^{-1} . The reaction first forms a complex 21 kJ mol^{-1} below the reactants but this rearranges to the products via a transition state that is 110 kJ mol^{-1} above the reactants.
R4.	$HOI + NO_3 \rightarrow IO + HNO_3$	Exothermic by 11 kJ mol^{-1} with all transition states below the reactants. $k(T) = 2.7 \times 10^{-12} (300 \text{ K} / T)^{2.66} \text{ cm}^3 \text{ molecule}^{-1} \text{ s}^{-1}$

5
6

1 **Table 2.** Calculated vibrational frequencies, rotational constants and energies of the stationary
 2 points and asymptotes on the HOI + NO₃ doublet potential energy surface

Species	Geometry ^a	Vibrational frequencies ^b	Rotational constants ^c	Potential energy ^d
HOI + NO ₃		603, 1084, 3803 & 261, 261, 805, 1108, 1108, 1126	623.9, 8.182, 8.076 & 13.84, 13.84, 6.919	0.0
IOH-NO ₃ complex	O 1.623, 0.284, -0.331 H 1.484, -0.657, -0.043 I 0.009, 1.205, 0.286 N -0.456, -2.265, 0.030 O -1.052, -3.321, -0.0473 O -1.147, -1.195, -0.228 O 0.742, -2.161, 0.333	55, 84, 118, 161, 196, 615, 629, 667, 705, 803, 968, 1228, 1273, 1491, 3268	5.610, 0.916, 0.806	-24.0
IO-H-NO ₂ TS	O 0.309, 1.515, 0.247 H -0.834, 1.314, -0.017 I 1.280, -0.089, -0.093 N -2.349, -0.133, 0.019 O -3.518, -0.429, -0.035 O -1.444, -0.962, 0.257 O -2.019, 1.117, -0.187	1249i, 70, 97, 103, 225, 472, 676, 698, 797, 806, 1041, 1147, 1308, 1513, 1626	6.300, 0.864, 0.767	-16.4
IO-HNO ₃ complex	O 0.571, 1.350, 0.348 H -1.111, 1.098, -0.020 I 1.870, 0.0645, -0.152 N -2.503, -0.202, 0.0186 O -3.673, -0.396, -0.170 O -1.654, -0.986, 0.401 O -2.081, 1.090, -0.242	35, 43, 76, 126, 198, 623, 677, 703, 772, 798, 939, 1331, 1416, 1713, 3281	7.058, 0.605, 0.566	-34.8
IO + HNO ₃		648 & 477, 585, 649, 782, 901, 1320, 1345, 1738, 3724	9.844 & 13.01, 12.05, 6.258	-10.6

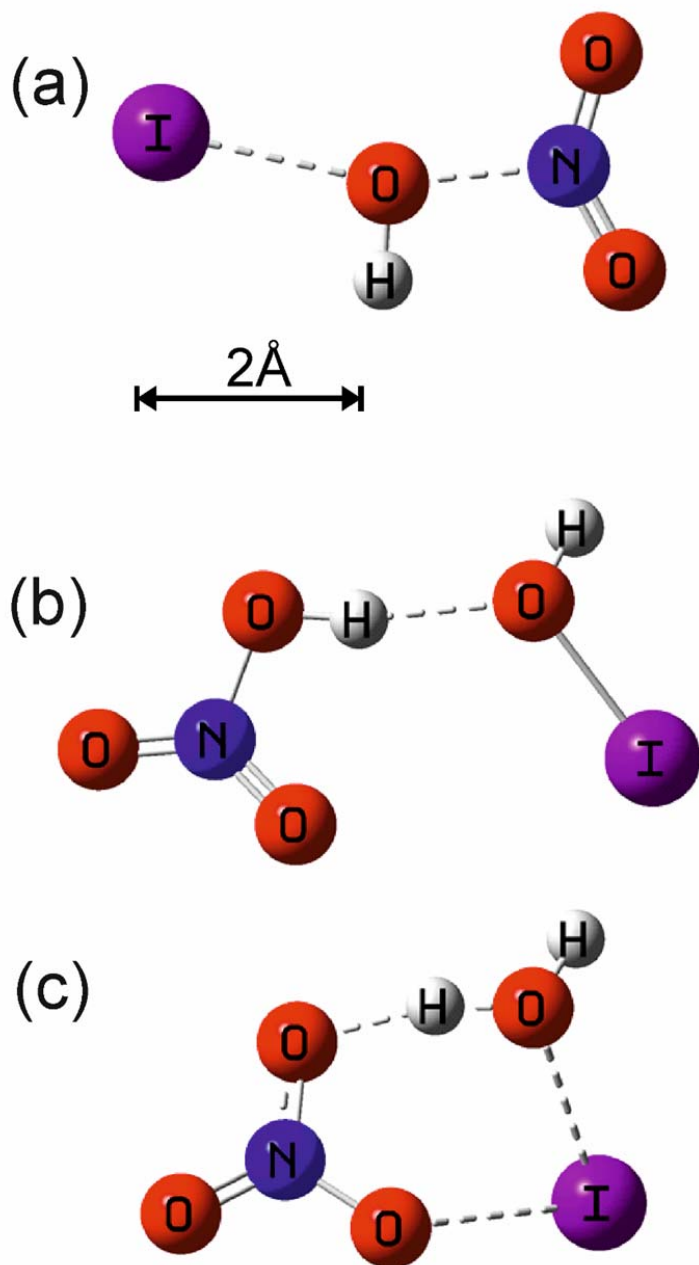
3 ^a Cartesian co-ordinates in Å. ^b In cm⁻¹. ^c In GHz. ^d In kJ mol⁻¹, including zero-point energy and spin-
 4 orbit coupling of I and IO (see text).



15 **Figure 1.** New nocturnal iodine chemistry (in white) implemented in the THAMO and CAM-
 16 Chem models.

17
 18
 19
 20
 21
 22
 23
 24
 25

1



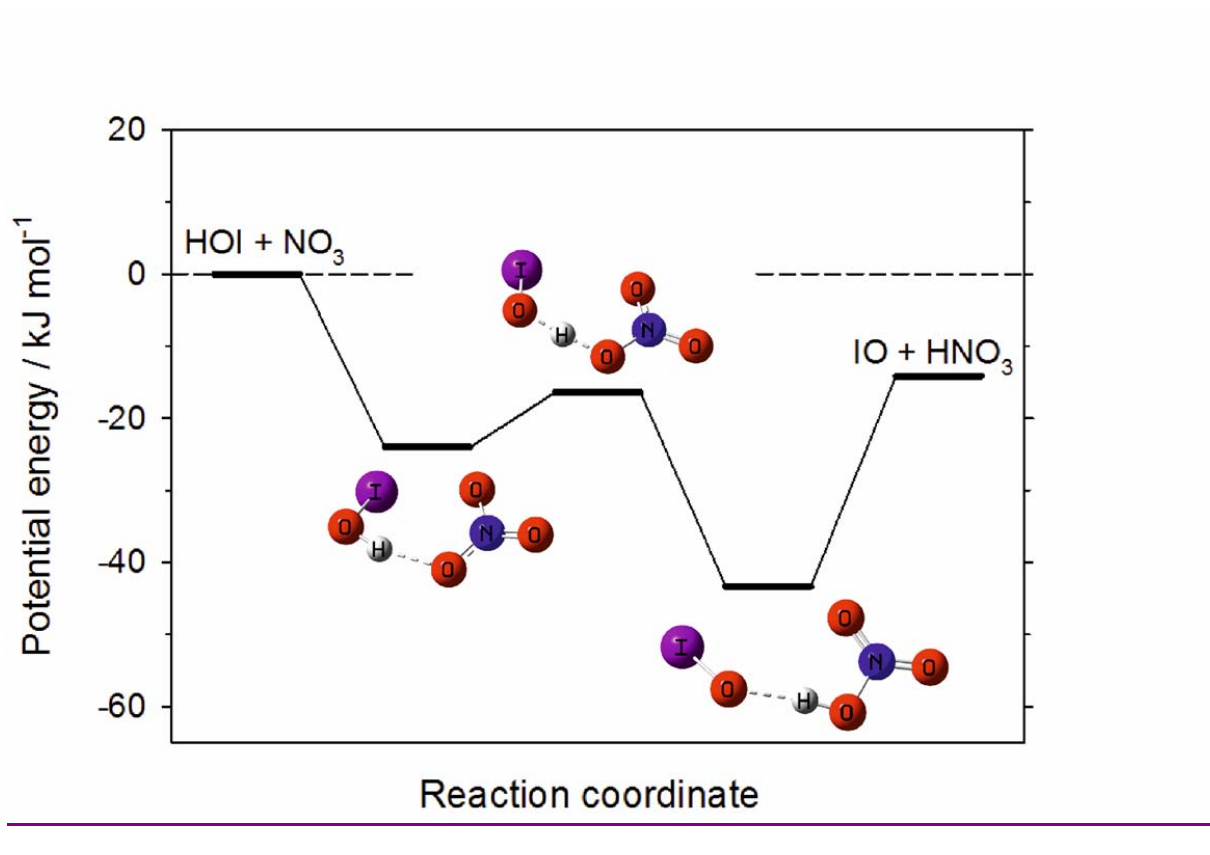
2

3

4

5 **Figure 2:** (a) Transition state for the reaction between HOI and NO₂ to form HNO₃ + I; (b)
6 complex formed between HOI and HNO₃, which then reacts via transition state (c) to form
7 IONO₂ + H₂O.

1

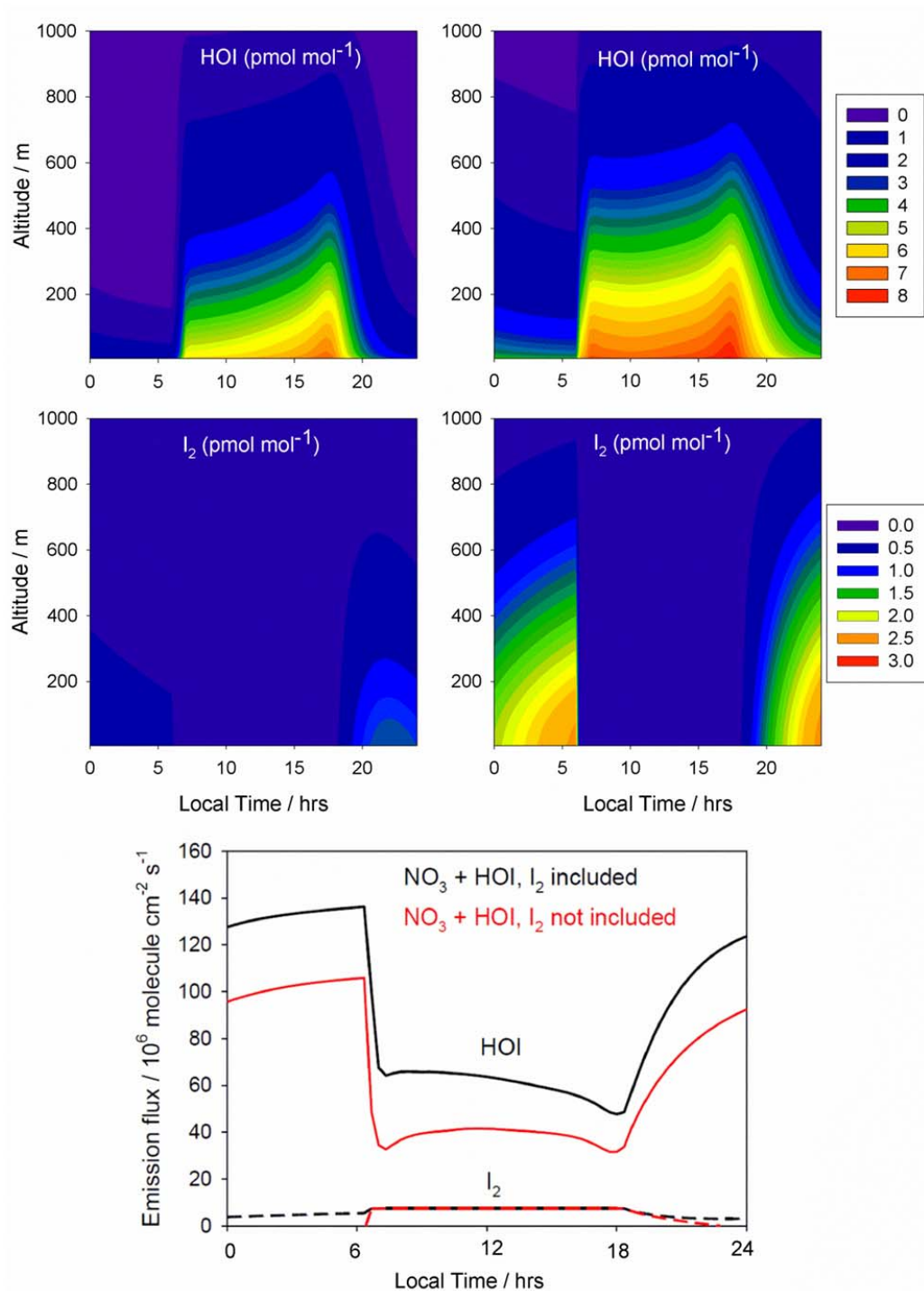


2

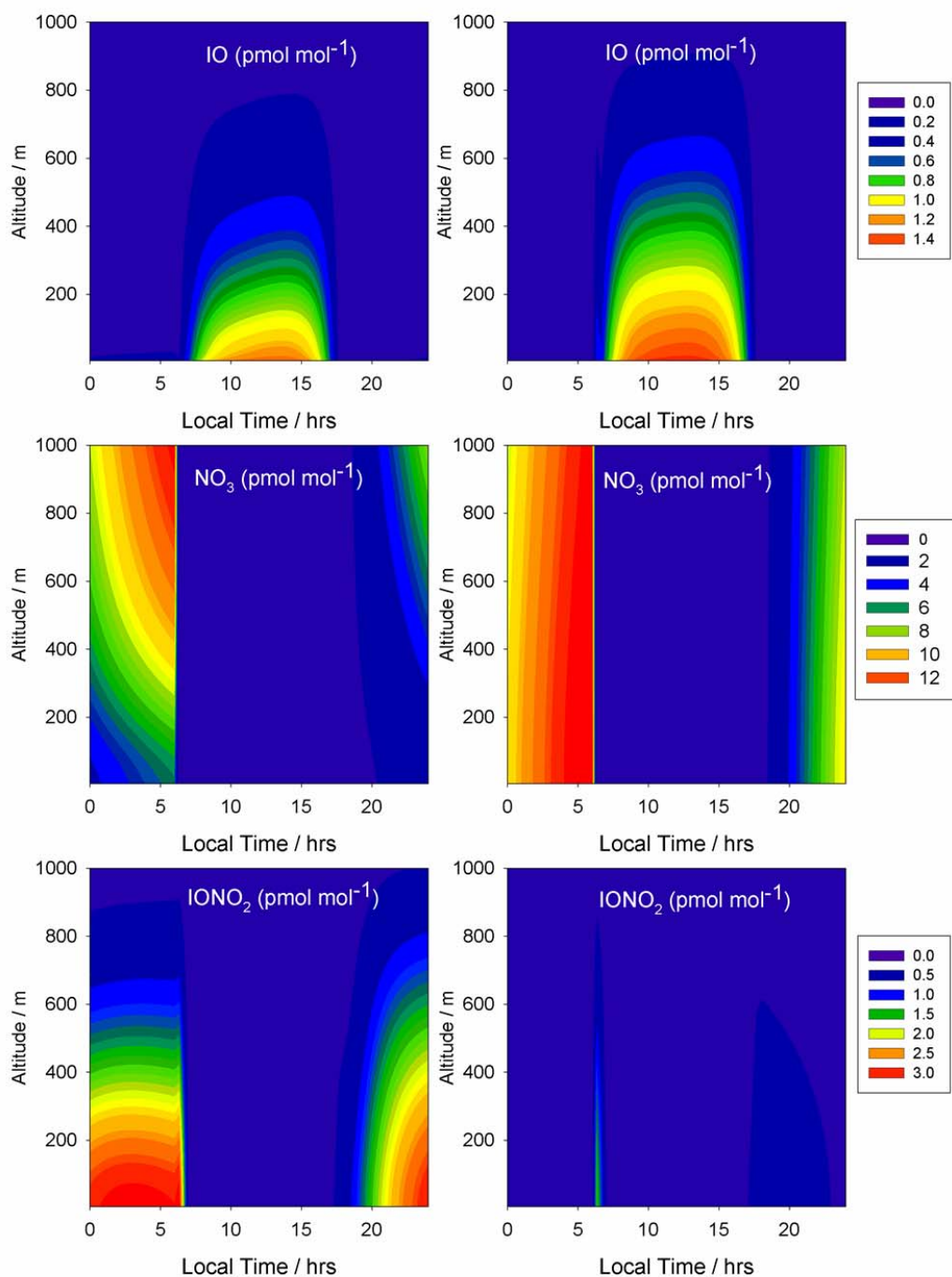
3

4 **Figure 3.** Potential energy surface for the reaction between HOI and NO₃, which contains two
5 intermediate complexes separated by a submerged barrier.

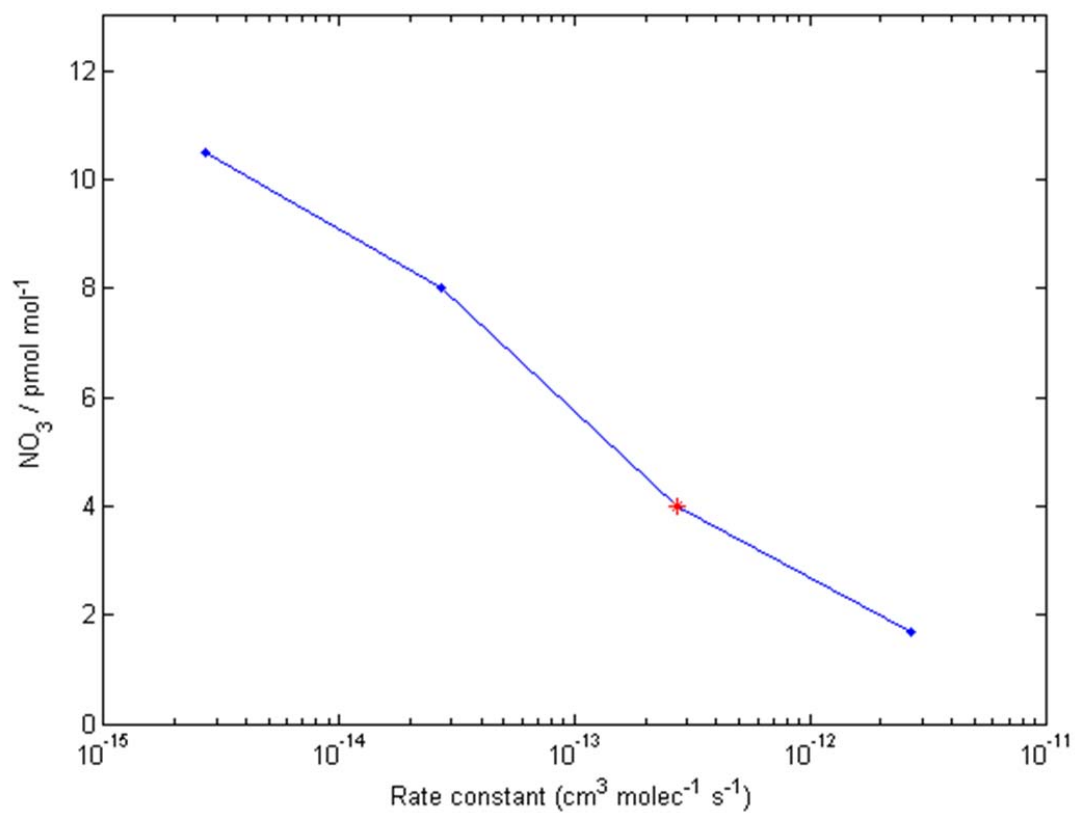
6



1
 2 **Figure 4.** THAMO modeled diurnal variation of HOI, I₂ (upper panels) and the HOI/I₂ flux from
 3 the ocean surface (bottom panel). The right hand panels are from scenario 1, which do not
 4 include night time reactions of HOI and I₂ with NO₃, while the left hand panels include the
 5 reactions in scenario 2. In bottom panel red lines represent scenario 1, while black lines
 6 correspond to scenario 2.



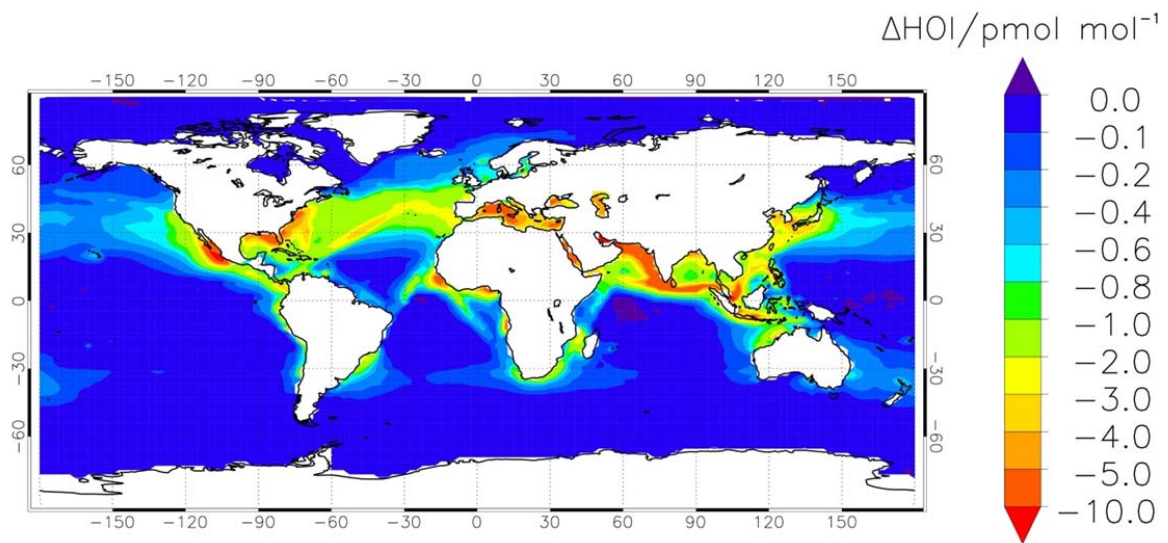
1
 2 **Figure 5.** THAMO modeled diurnal variation of IO, NO₃ and the IONO₂. The right hand panels
 3 are from scenario 1, which do not include night time reactions of HOI and I₂ with NO₃, while the
 4 left hand panels include the reactions in scenario 2.



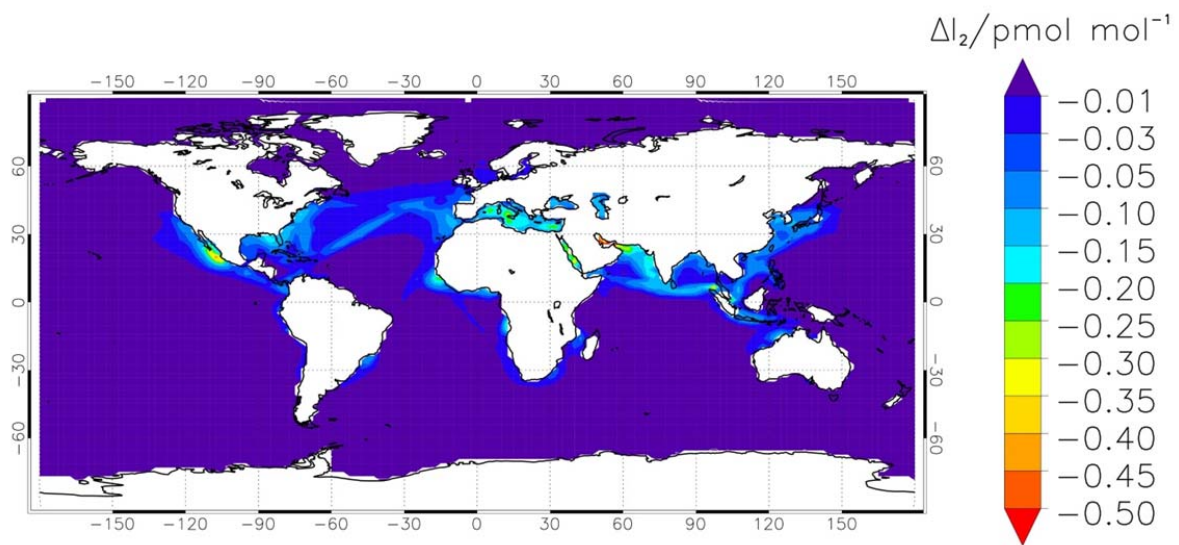
1
2 **Figure 6.** Sensitivity run showing the effect of the uncertainty in the rate constant estimation on
3 the reduction of NO_3 [peak nighttime concentration](#) at the surface - the red point is the theoretical
4 estimate.

5
6
7
8
9
10
11

1



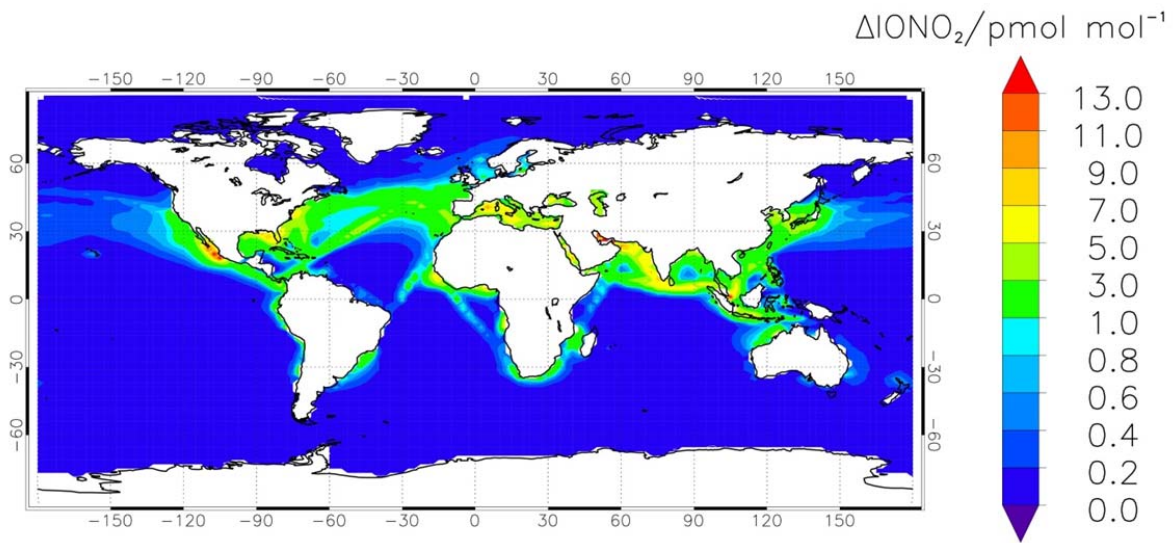
2



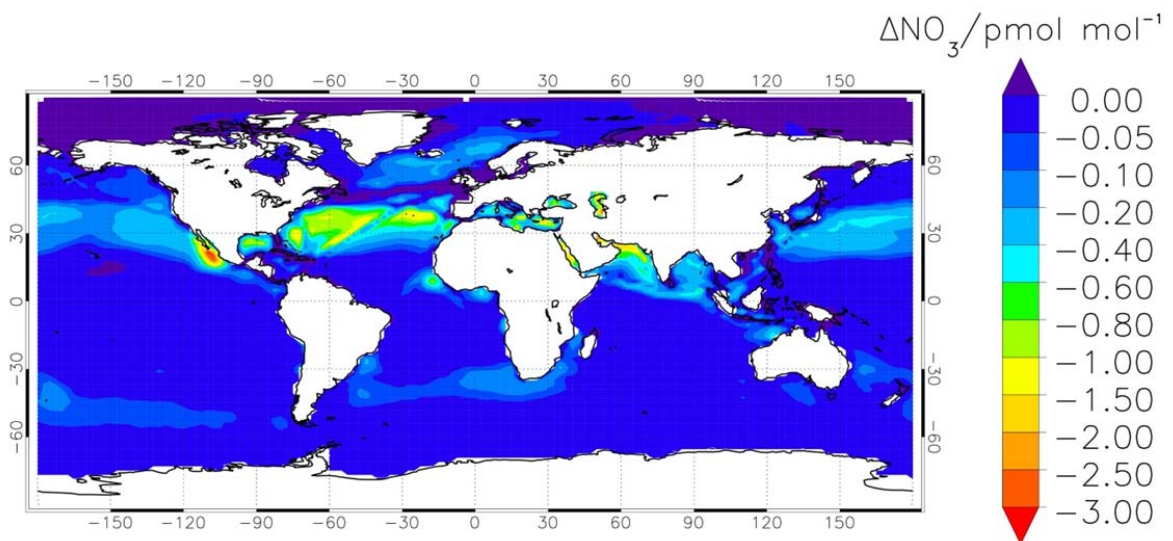
3

4 | **Figure 7.** Modelled annual average of HOI (a) and I₂ (b) during night time (from 0:00 to 1:00
5 | [LT](#)) at the surface level. The panels show the difference in volume mixing ratio between the
6 | simulations with and without reactions (1) and (4).

7



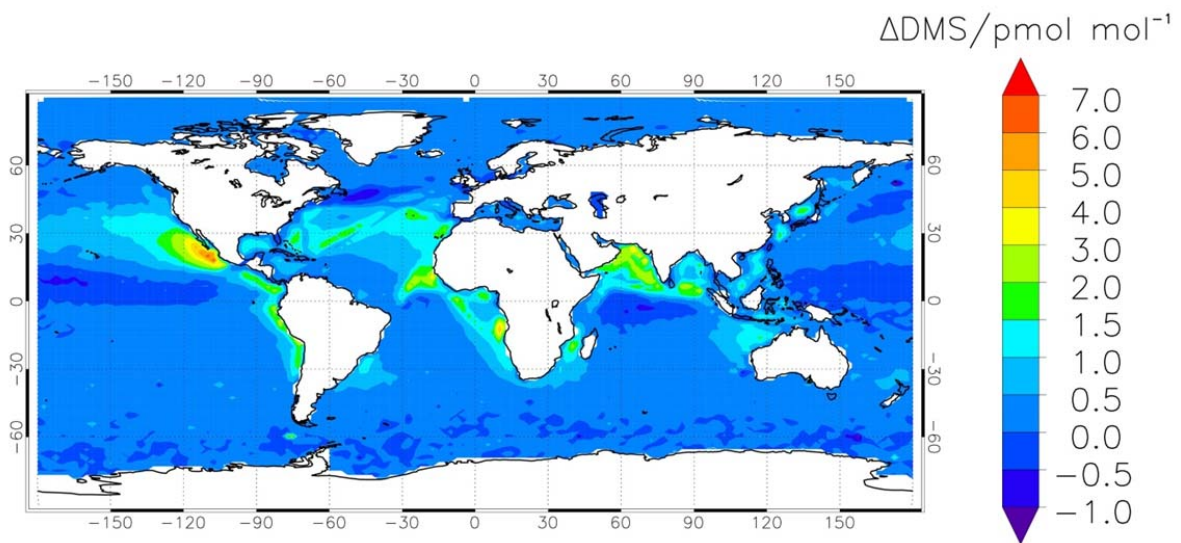
1



2

3 **Figure 8.** Modelled annual average of IONO_2 (a) and NO_3 (b) during night time ([from 0:00 to](#)
 4 [1:00 LT](#)) at the surface level, as the difference in volume mixing ratio between the simulations
 5 with and without reactions (1) and (4).

6



1

2 | **Figure 9.** Increase in the DMS levels during night time (from 0:00 to 1:00 LT) at the surface
 3 level due to the inclusion of the reactions R1 and R4 in CAM-Chem.

4

5

6

7

8

9

10

11

12

13

14

15

16

1
2
3
4
5
6
7
8
9
10
11
12
13
14
15
16
17
18
19
20
21
22
23
24

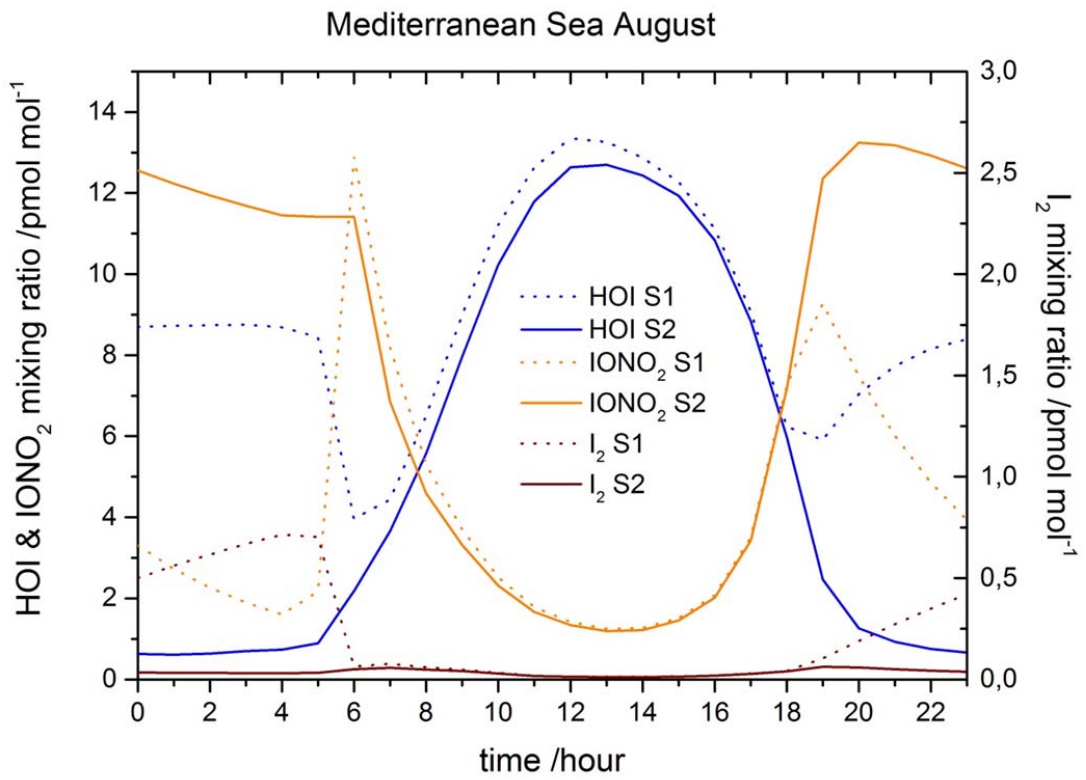
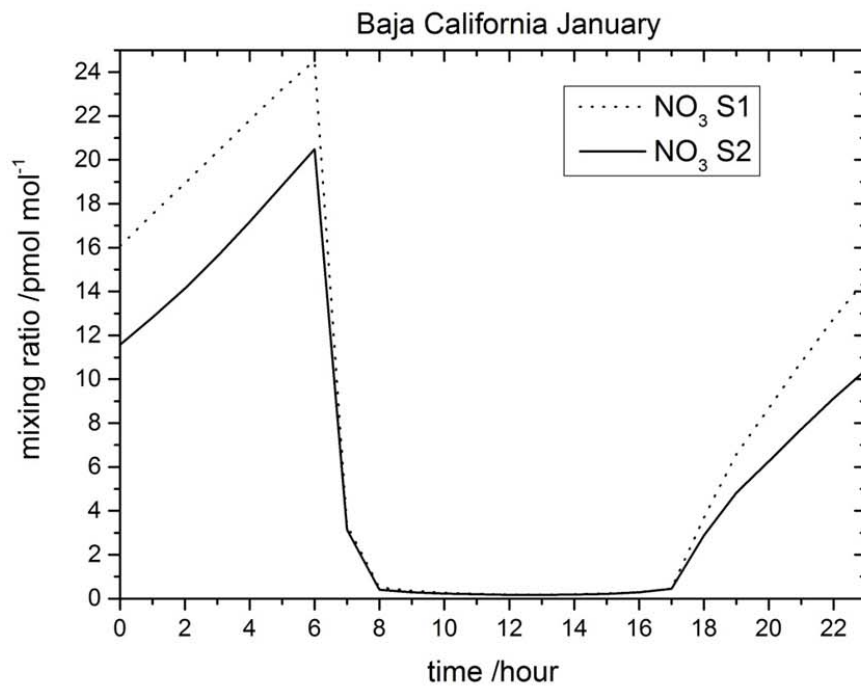
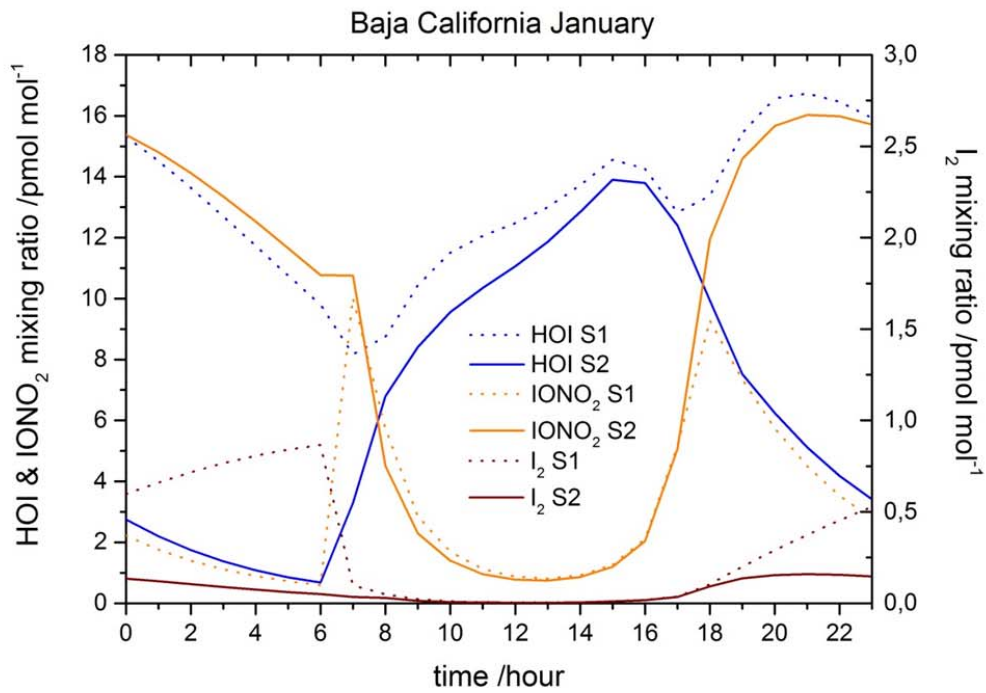


Figure 10. Hourly averaged concentration of HOI, IONO₂ and I₂ in the Mediterranean Sea at the surface level (lon:10°→20°E, lat:33°→40°N)



22 **Figure 11.** Hourly averaged concentration of HOI, IONO₂ and I₂ (upper panel) and NO₃ (bottom
 23 panel) in the Pacific Ocean at the south of Baja California peninsula at the surface level
 24 (lon: -110°→-106°E, lat:16°→23°N)

Supplementary information for

Nighttime atmospheric chemistry of iodine

Alfonso Saiz-Lopez¹, John M.C. Plane², Carlos A. Cuevas¹, Anoop S. Mahajan³,
Jean-François Lamarque⁴ and Douglas E. Kinnison⁴

¹Department of Atmospheric Chemistry and Climate, Institute of Physical Chemistry Rocasolano, CSIC, Madrid, Spain

²School of Chemistry, University of Leeds, Leeds, UK

³Indian Institute of Tropical Meteorology, Pune, India

⁴Atmospheric Chemistry Observations and Modelling, NCAR, Colorado, USA

Correspondence to: A. Saiz-Lopez (a.saiz@csic.es)

Table 1. Iodine chemistry scheme in CAM-Chem: Bimolecular, thermal decomposition and termolecular reactions.

Reaction	$k / \text{cm}^3 \text{ molecule}^{-1} \text{ s}^{-1}$	Notes
$\text{I} + \text{O}_3 \rightarrow \text{IO} + \text{O}_2$	$2.1 \times 10^{-11} e^{(-830/T)}$	1
$\text{IO} + \text{O}_3 \rightarrow \text{OIO} + \text{O}_2$	3.6×10^{-16}	2
$\text{I} + \text{HO}_2 \rightarrow \text{HI} + \text{O}_2$	$1.5 \times 10^{-11} e^{(-1090/T)}$	3
$\text{IO} + \text{NO} \rightarrow \text{I} + \text{NO}_2$	$7.15 \times 10^{-12} e^{(300/T)}$	1
$\text{IO} + \text{HO}_2 \rightarrow \text{HOI} + \text{O}_2$	$1.4 \times 10^{-11} e^{(540/T)}$	1
$\text{IO} + \text{IO} \rightarrow \text{OIO} + \text{I}$	$2.13 \times 10^{-11} e^{(180/T)} \times [1 + e^{(p/191.42)}]$	1, 4
$\text{IO} + \text{IO} \rightarrow \text{I}_2\text{O}_2$	$3.27 \times 10^{-11} e^{(180/T)} \times [1 - 0.65 e^{(-p/191.42)}]$	1, 4
$\text{IO} + \text{OIO} \rightarrow \text{I}_2\text{O}_3$	$w_1 \cdot \exp(w_2 \cdot T)^a$	4, 5, 6 ^g
$\text{OIO} + \text{OIO} \rightarrow \text{I}_2\text{O}_4$	$w_1 \cdot \exp(w_2 \cdot T)^b$	4, 5, 6 ^g
$\text{I}_2 + \text{O} \rightarrow \text{IO} + \text{I}$	1.25×10^{-10}	1
$\text{IO} + \text{O} \rightarrow \text{I} + \text{O}_2$	1.4×10^{-10}	1
$\text{IO} + \text{OH} \rightarrow \text{HO}_2 + \text{I}$	1.0×10^{-10}	7
$\text{I}_2\text{O}_2 \rightarrow \text{OIO} + \text{I}$	$w_1 \cdot \exp(w_2/T)^c$	5, 6, 8 ^g
$\text{I}_2\text{O}_2 \rightarrow \text{IO} + \text{IO}$	$w_1 \cdot \exp(w_2/T)^d$	5, 6, 8 ^g
$\text{I}_2\text{O}_4 \rightarrow 2 \text{OIO}$	$w_1 \cdot \exp(w_2/T)^e$	5, 8 ^g
$\text{I}_2 + \text{OH} \rightarrow \text{HOI} + \text{I}$	1.8×10^{-10}	3
$\text{I}_2 + \text{NO}_3 \rightarrow \text{I} + \text{IONO}_2$	1.5×10^{-12}	9
$\text{I} + \text{NO}_3 \rightarrow \text{IO} + \text{NO}_2$	1.0×10^{-10}	1
$\text{OH} + \text{HI} \rightarrow \text{I} + \text{H}_2\text{O}$	$1.6 \times 10^{-11} e^{(440/T)}$	1
$\text{I} + \text{IONO}_2 \rightarrow \text{I}_2 + \text{NO}_3$	$9.1 \times 10^{-11} e^{(-146/T)}$	5
$\text{HOI} + \text{OH} \rightarrow \text{IO} + \text{H}_2\text{O}$	2.0×10^{-13}	10
$\text{IO} + \text{DMS} \rightarrow \text{DMSO} + \text{I}$	$3.2 \times 10^{-13} e^{(-925/T)}$	11
$\text{INO}_2 \rightarrow \text{I} + \text{NO}_2$	$1008 \times 10^{15} e^{(-13670/T)}$	12, 13, 14
$\text{IONO}_2 \rightarrow \text{IO} + \text{NO}_2$	$w_1 \cdot \exp(w_2/T)^f$	5, 15
$\text{INO} + \text{INO} \rightarrow \text{I}_2 + 2\text{NO}$	$8.4 \times 10^{-11} e^{(-2620/T)}$	3
$\text{INO}_2 + \text{INO}_2 \rightarrow \text{I}_2 + 2\text{NO}_2$	$4.7 \times 10^{-13} e^{(-1670/T)}$	1
$\text{OIO} + \text{NO} \rightarrow \text{IO} + \text{NO}_2$	$1.1 \times 10^{-12} e^{(542/T)}$	14
$\text{HI} + \text{NO}_3 \rightarrow \text{I} + \text{HNO}_3$	$1.3 \times 10^{-12} e^{(-1830/T)}$	16
$\text{IO} + \text{BrO} \rightarrow \text{Br} + \text{I} + \text{O}_2$	$0.30 \times 10^{-11} e^{(510/T)}$	1
$\text{IO} + \text{BrO} \rightarrow \text{Br} + \text{OIO}$	$1.20 \times 10^{-11} e^{(510/T)}$	1
$\text{I} + \text{BrO} \rightarrow \text{IO} + \text{Br}$	1.44×10^{-11}	17, 18, 19

IO + ClO → I + OCIO	$2.585 \times 10^{-12} e^{(280/T)}$	1
IO + ClO → I + Cl + O ₂	$1.175 \times 10^{-12} e^{(280/T)}$	1
IO + ClO → ICl + O ₂	$0.940 \times 10^{-12} e^{(280/T)}$	1
IO + Br → I + BrO	2.49×10^{-11}	18, 19
IO + NO ₃ → OIO + NO ₂	9.0×10^{-12}	20
IO + CH ₃ O ₂ → CH ₂ O + I + HO ₂	2.0×10^{-12}	2 ^h
CH ₃ I + OH → I + H ₂ O + HO ₂	$2.90 \times 10^{-12} e^{(-1100/T)}$	3
I + NO ₂ (+ M) → INO ₂ (+ M)	$k_0 = 3 \times 10^{-31} \times (T / 300)^{-1}$ $k_\infty = 6.6 \times 10^{-11}$	3 ⁱ
IO + NO ₂ (+ M) → IONO ₂ (+ M)	$k_0 = 6.5 \times 10^{-31} \times (T / 300)^{-3.5}$ $k_\infty = 7.6 \times 10^{-12} \times (T / 300)^{-1.5}$	3 ⁱ
I + NO (+ M) → INO (+ M)	$k_0 = 1.8 \times 10^{-32} \times (T / 300)^{-1}$ $k_\infty = 1.7 \times 10^{-11}$	3 ⁱ
OIO + OH (+ M) → HOIO ₂ (+ M)	$k_0 = 1.5 \times 10^{-27} \times (T / 300)^{-3.93}$ $k_\infty = 7.76 \times 10^{-10} \times (T / 300)^{-0.8}$	14 ^j
HOI + NO ₃ → IO + HNO ₃	$2.7 \times 10^{-12} (300/T)^{2.66}$	21

¹ IUPAC-2008 (Atkinson et al., 2007) ; ²(Dillon et al., 2006b); ³ JPL-2010 (Sander et al., 2011); ⁴(Gómez Martín et al., 2007); ⁵(Kaltsoyannis and Plane, 2008); ⁶(Galvez et al., 2013); ⁷(Bösch et al., 2003); ⁸ (Gómez Martín and Plane, 2009); ⁹(Chambers et al., 1992); ¹⁰(Chameides and Davis, 1980); ¹¹(Dillon et al., 2006a); ¹²(McFiggans et al., 2000); ¹³(Jenkin et al., 1985); ¹⁴(Plane et al., 2006); ¹⁵(Allan and Plane, 2002); ¹⁶(Lancar et al., 1991); ¹⁷(Laszlo et al., 1997); ¹⁸(Bedjanian et al., 1997); ¹⁹(Gilles et al., 1997); ²⁰(Dillon et al., 2008); ²¹This work.

$$^a \quad w1 = 4.687 \times 10^{-10} - 1.3855 \times 10^{-5} \times e^{(-0.75 \text{ p} / 1.62265)} + 5.51868 \times 10^{-10} \times e^{(-0.75 \text{ p} / 199.328)}$$

$$w2 = -0.00331 - 0.00514 \times e^{(-0.75 \text{ p} / 325.68711)} - 0.00444 \times e^{(-0.75 \text{ p} / 40.81609)}$$

$$^b \quad w1 = 1.1659 \times 10^{-9} - 7.79644 \times 10^{-10} \times e^{(-0.75 \text{ p} / 22.09281)} + 1.03779 \times 10^{-9} \times e^{(-0.75 \text{ p} / 568.15381)}$$

$$w2 = -0.00813 - 0.00382 \times e^{(-0.75 \text{ p} / 45.57591)} - 0.00643 \times e^{(-0.75 \text{ p} / 417.95061)}$$

$$^c \quad w1 = 3.54288 \times 10^{10} + 1.8523 \times 10^{11} \times 0.75 \text{ p} - 1.45435 \times 10^8 \times (0.75 \text{ p})^2 + 60799.4344 \times (0.75 \text{ p})^3$$

$$w2 = -9681.65989 + 346.95538 \times e^{(-0.75 \text{ p} / 343.25322)} + 251.78032 \times e^{(-0.75 \text{ p} / 44.1466)}$$

$$^d \quad w1 = 255335000000 - 4418880000 \times 0.75 \text{ p} + 85618600 \times (0.75 \text{ p})^2 + 14218.81 \times (0.75 \text{ p})^3$$

$$w2 = -11466.82304 + 597.01334 \times e^{(-0.75 \text{ p} / 1382.62325)} - 167.3391 \times e^{(-0.75 \text{ p} / 43.75089)}$$

$$^e \quad w1 = -1.92626 \times 10^{14} + 4.67414 \times 10^{13} \times 0.75 \text{ p} - 3.68651 \times 10^8 \times (0.75 \text{ p})^2 - 3.09109 \times 10^6 \times (0.75 \text{ p})^3$$

$$w2 = -12302.15294 + 252.78367 \times e^{(-0.75 \text{ p} / 46.12733)} + 437.62868 \times e^{(-0.75 \text{ p} / 428.4413)}$$

$$\begin{aligned}
 {}^f \quad w_1 &= -2.63544 \times 10^{13} + 4.32845 \times 10^{12} \times (0.75 \text{ p}) + 3.73758 \times 10^8 \times (0.75 \text{ p})^2 - \\
 &628468.76313 \times (0.75 \text{ p})^3 \\
 w_2 &= -13847.85015 + 240.34465 \times e^{(-0.75 \text{ p} / 49.27141)} + 451.35864 \times e^{(-0.75 \text{ p} / \\
 &436.87605)}
 \end{aligned}$$

^g The empirical expressions of the form $w_1 \cdot \exp(w_2 \cdot T)$ were obtained by non-linear least squares fitting of *Rice–Ramsperger–Kassel–Marcus* (RRKM) theoretical results for the indicated reaction rate constants and thermal dissociation rates in the (27 – 1013) hPa pressure range. RRKM calculations were carried out using the MESMER algorithm (Glowacki et al., 2012) as indicated in the corresponding references (e.g. (Galvez et al., 2013)). Expression ^a produces negative values outside the range of modelled rate constants ($p < 20$ hPa), and therefore a fixed rate constant of $3 \times 10^{-11} \text{ cm}^3 \text{ molecule}^{-1} \text{ s}^{-1}$ was assumed. Expressions ^e and ^f generate negligible dissociation rates below ~ 500 hPa which become negative at ~ 8 hPa – in this case they are set to zero below that pressure.

^h Updated heats of formation for IO, OIO, and CH_3O_2 (Dooley et al., 2008; Gómez Martín and Plane, 2009; Knyazev and Slagle, 1998) show that the only accessible exothermic product channel of $\text{CH}_3\text{O}_2 + \text{IO}$ (Drougas and Kosmas, 2007) is $\text{CH}_2\text{O} + \text{I} + \text{O}_2$ ($\Delta H_r = -5 \pm 6 \text{ kJ mol}^{-1}$), consistent with the high yield of I and low yield of OIO found experimentally (Bale et al., 2005; Enami et al., 2006). Sensitivity studies have been carried out (Saiz-Lopez et al., 2014) using the preferred rate constant for this reaction of $2 \times 10^{-12} \text{ cm}^3 \text{ molecule}^{-1} \text{ s}^{-1}$ (Dillon et al., 2006b), resulting in an enhancement of the ozone loss of 0.5% in the MBL and of less than 0.1% integrated throughout the troposphere in the $J_{\text{I}_x\text{O}_y}$ scenario, and similarly negligible enhancements in the Base scenario. Impacts in the I_y partitioning are also very minor.

ⁱ The temperature and pressure dependent rate constant (k) is computed based on the low pressure (k_0) and the high-pressure (k_∞) rate coefficients following JPL-2010 (Sander et al., 2011).

^j The Fast rate constants and a thermally stable product HOIO_2 have been predicted theoretically (Plane et al., 2006), but no experimental studies reporting observation of HOIO_2 and its photochemical properties in the gas phase are available. Since the level of uncertainty is even larger than for the I_xO_y , it has not been included in the mechanism.

Table 2. Iodine chemistry scheme in CAM-Chem: Photochemical reactions.

Reaction
$\text{CH}_3\text{I} + h\nu \rightarrow \text{CH}_3\text{O}_2 + \text{I}$
$\text{CH}_2\text{I}_2 + h\nu \rightarrow 2\text{I}^a$
$\text{CH}_2\text{IBr} + h\nu \rightarrow \text{Br} + \text{I}^a$
$\text{CH}_2\text{ICl} + h\nu \rightarrow \text{Cl} + \text{I}^a$
$\text{I}_2 + h\nu \rightarrow 2\text{I}$
$\text{IO} + h\nu \rightarrow \text{I} + \text{O}$
$\text{OIO} + h\nu \rightarrow \text{I} + \text{O}_2$
$\text{INO} + h\nu \rightarrow \text{I} + \text{NO}$
$\text{INO}_2 + h\nu \rightarrow \text{I} + \text{NO}_2^b$
$\text{IONO}_2 + h\nu \rightarrow \text{I} + \text{NO}_3$
$\text{HOI} + h\nu \rightarrow \text{I} + \text{OH}$
$\text{IBr} + h\nu \rightarrow \text{I} + \text{Br}$
$\text{ICl} + h\nu \rightarrow \text{I} + \text{Cl}$
$\text{I}_2\text{O}_2 + h\nu \rightarrow \text{I} + \text{OIO}^c$
$\text{I}_2\text{O}_3 + h\nu \rightarrow \text{IO} + \text{OIO}^c$
$\text{I}_2\text{O}_4 + h\nu \rightarrow \text{OIO} + \text{OIO}^c$

Photolysis rates are computed online considering the actinic flux calculation in CAM-Chem. The absorption cross-sections and quantum yields for all species besides the I_xO_y have been taken from IUPAC-2008 (Atkinson et al., 2007; Atkinson et al., 2008) and JPL-2010 (Sander et al., 2011).

^a radical organic products are not considered.

^b only the reaction channel reported in JPL 06-02 (Sander et al., 2006) is considered.

^c photolysis reactions only considered in the $J_{\text{I}x\text{O}y}$ scheme (Saiz-Lopez et al., 2014).

Table 3. Iodine chemistry scheme in CAM-Chem: Heterogeneous reactions.

Sea-salt aerosol reactions	Reactive uptake
$\text{IONO}_2 \rightarrow 0.5 \text{ IBr} + 0.5 \text{ ICl}$	$\gamma = 0.01$
$\text{INO}_2 \rightarrow 0.5 \text{ IBr} + 0.5 \text{ ICl}$	$\gamma = 0.02$
$\text{HOI} \rightarrow 0.5 \text{ IBr} + 0.5 \text{ ICl}$	$\gamma = 0.06$
$\text{I}_2\text{O}_2 \rightarrow$	$\gamma = 0.01^{\S}$
$\text{I}_2\text{O}_3 \rightarrow$	$\gamma = 0.01^{\S}$
$\text{I}_2\text{O}_4 \rightarrow$	$\gamma = 0.01^{\S}$

Values based on the THAMO model (Saiz-Lopez et al., 2008) and implemented in CAM-Chem following (Ordóñez et al., 2012).

[§] Deposition of I_xO_y species on sea-salt aerosols has been included following the free regime approximation.

Table 4. Iodine chemistry scheme in CAM-Chem: Henry's Law constants and dry deposition velocities.

Species	k_0 (M atm ⁻¹)	Deposition velocity [§] (cm s ⁻¹)	Reference
IBr ^{ice}	2.4×10^1	–	1
ICl ^{ice}	1.1×10^2	–	1
HI	7.8×10^{-1}	1.0	1 ^a
HOI – ($J_{I_xO_y} / Base$)	$1.9 \times 10^3 / 4.5 \times 10^3$	0.75	1 ^b
IONO ₂ ^{ice}	1.0×10^6	0.75	2 ^c
INO ₂ ^{ice}	3.0×10^{-1}	0.75	1 ^d
IO	4.5×10^2	–	2
OIO	1.0×10^4	–	2
I ₂ O ₂	1.0×10^4	1.0	2
I ₂ O ₃	1.0×10^4	1.0	2
I ₂ O ₄	1.0×10^4	1.0	2

[§] Dry deposition velocities are based on the THAMO model (Saiz-Lopez et al., 2008).

¹ Values reported in (Sander, 1999).

² Values based on the THAMO model (Saiz-Lopez et al., 2008).

^a Considering a dissociation constant $K_a = 3.2 \times 10^9$ and a temperature dependent coefficient $c = 9800$ K

^b Within the range of values given in the corresponding reference.

^c Virtually infinite solubility is represented by using a very large arbitrary number.

^d Value assumed to be equal to those of BrNO₂.

^{ice} Species for which ice-uptake is considered following (Neu and Prather, 2012).

References

Allan, B. J., and Plane, J. M. C.: A Study of the Recombination of IO with NO₂ and the Stability of INO₃: Implications for the Atmospheric Chemistry of Iodine, *J. Phys. Chem. A*, 106, 8634-8641, 2002.

Atkinson, R., Baulch, D. L., Cox, R. A., Crowley, J. N., Hampson, R. F., Hynes, R. G., Jenkin, M. E., Rossi, M. J., and Troe, J.: Evaluated kinetic and photochemical data for atmospheric chemistry: Volume III: gas phase reactions of inorganic halogens, *Atmos. Chem. Phys.*, 7, 981-1191, 2007.

Atkinson, R., Baulch, D. L., Cox, R. A., Crowley, J. N., Hampson, R. F., Hynes, R. G., Jenkin, M. E., Rossi, M. J., Troe, J., and Wallington, T. J.: Evaluated kinetic and photochemical data for atmospheric chemistry: Volume IV – gas phase reactions of organic halogen species, *Atmos. Chem. Phys.*, 8, 4141-4496, 10.5194/acp-8-4141-2008, 2008.

- Bale, C. S. E., Canosa-Mas, C. E., Shallcross, D. E., and Wayne, R. P.: A discharge-flow study of the kinetics of the reactions of IO with CH₃O₂ and CF₃O₂, *Phys. Chem. Chem. Phys.*, 7, 2164-2172, 2005.
- Bedjanian, Y., Le Bras, G., and Poulet, G.: Kinetic study of the Br + IO, I + BrO and Br + I₂ reactions. Heat of formation of the BrO radical, *Chem. Phys. Lett.*, 266, 233-238, doi: 10.1016/S0009-2614(97)01530-3, 1997.
- Bösch, H., Camy-Peyret, C., Chipperfield, M. P., Fitzenberger, R., Harder, H., Platt, U., and Pfeilsticker, K.: Upper limits of stratospheric IO and OIO inferred from center-to-limb-darkening-corrected balloon-borne solar occultation visible spectra: Implications for total gaseous iodine and stratospheric ozone, *J. Geophys. Res.*, 108, 4455, 2003.
- Chambers, R. M., Heard, A. C., and Wayne, R. P.: Inorganic gas-phase reactions of the nitrate radical: iodine + nitrate radical and iodine atom + nitrate radical, *J. Phys. Chem.*, 96, 3321-3331, 10.1021/j100187a028, 1992.
- Chameides, W. L., and Davis, D.: Iodine: Its Possible Role in Tropospheric Photochemistry, *J. Geophys. Res.*, 85, 7383-7398, 1980.
- Dillon, T. J., Karunanandan, R., and Crowley, J. N.: The reaction of IO with CH₃SCH₃: products and temperature dependent rate coefficients by laser induced fluorescence, *Phys. Chem. Chem. Phys.*, 8, 847-855, 2006a.
- Dillon, T. J., Tucceri, M. E., and Crowley, J. N.: Laser induced fluorescence studies of iodine oxide chemistry Part II. The reactions of IO with CH₃O₂, CF₃O₂ and O₃., *Phys. Chem. Chem. Phys.*, 8, 5185-5198, 2006b.
- Dillon, T. J., Tucceri, M. E., Sander, R., and Crowley, J. N.: LIF studies of iodine oxide chemistry Part 3. Reactions IO + NO₃ -> OIO + NO₂, I + NO₃ -> IO + NO₂, and CH₂I + O₂ -> (products): implications for the chemistry of the marine atmosphere at night., *Phys. Chem. Chem. Phys.*, 10, 1540-1554, 2008.
- Dooley, K. S., Geidosch, J. N., and North, S. W.: Ion imaging study of IO radical photodissociation: Accurate bond dissociation energy determination, *Chem. Phys. Lett.*, 457, 303-306, 2008.
- Drougas, E., and Kosmas, A. M.: Ab Initio Characterization of (CH₃IO₃) Isomers and the CH₃O₂ + IO Reaction Pathways, *J. Phys. Chem. A*, 111, 3402-3408, 2007.
- Enami, S., Yamanaka, T., Hashimoto, S., Kawasaki, M., Nakano, Y., and Ishiwata, T.: Kinetic Study of IO Radical with RO₂ (R = CH₃, C₂H₅, and CF₃) Using Cavity Ring-Down Spectroscopy, *J. Phys. Chem. A*, 110, 9861-9866, 2006.
- Galvez, O., Gomez Martin, J. C., Gomez, P. C., Saiz-Lopez, A., and Pacios, L. F.: A theoretical study on the formation of iodine oxide aggregates and monohydrates, *Phys. Chem. Chem. Phys.*, 15, 15572-15583, 10.1039/C3CP51219C, 2013.
- Gilles, M. K., Turnipseed, A. A., Burkholder, J. B., and Ravishankara, A. R.: A study of the Br + IO → I + BrO and the reverse reaction, *Chem. Phys. Lett.*, 272, 75-82, doi: 10.1016/S0009-2614(97)00485-5, 1997.
- Glowacki, D. R., Liang, C.-H., Morley, C., Pilling, M. J., and Robertson, S. H.: MESMER: An Open-Source Master Equation Solver for Multi-Energy Well Reactions, *J. Phys. Chem. A*, 116, 9545-9560, 10.1021/jp3051033, 2012.
- Gómez Martín, J. C., Spietz, P., and Burrows, J. P.: Kinetic and Mechanistic Studies of the I₂/O₃ Photochemistry, *J. Phys. Chem. A*, 111, 306-320, 2007.

- Gómez Martín, J. C., and Plane, J. M. C.: Determination of the O-IO bond dissociation energy by photofragment excitation spectroscopy, *Chem. Phys. Lett.*, 474, 79-83, 2009.
- Jenkin, M. E., Cox, R. A., and Candeland, D. E.: Photochemical Aspects of Tropospheric Iodine Behavior, *J. Atmos. Chem.*, 2, 359-375, 1985.
- Kaltsoyannis, N., and Plane, J. M. C.: Quantum chemical calculations on a selection of iodine-containing species (IO, OIO, INO_3 , $(\text{IO})_2$, I_2O_3 , I_2O_4 and I_2O_5) of importance in the atmosphere., *Phys. Chem. Chem. Phys.*, 10, 1723-1733, 2008.
- Knyazev, V. D., and Slagle, I. R.: Thermochemistry of the R-O2 Bond in Alkyl and Chloroalkyl Peroxy Radicals, *J. Phys. Chem. A*, 102, 1770-1778, 10.1021/jp9726091, 1998.
- Lancar, I. T., Mellouki, A., and Poulet, G.: Kinetics of the reactions of hydrogen iodide with hydroxyl and nitrate radicals, *Chem. Phys. Lett.*, 177, 554-558, 1991.
- Laszlo, B., Huie, R. E., Kurylo, M. J., and Miziolek, A. W.: Kinetic studies of the reactions of BrO and IO radicals, *J. Geophys. Res.*, 102, 1997.
- McFiggans, G., Plane, J. M. C., Allan, B. J., Carpenter, L. J., Coe, H., and O'Dowd, C.: A modeling study of iodine chemistry in the marine boundary layer, *J. Geophys. Res.*, [Atmos.], 105, 14371-14385, 2000.
- Neu, J. L., and Prather, M. J.: Toward a more physical representation of precipitation scavenging in global chemistry models: cloud overlap and ice physics and their impact on tropospheric ozone, *Atmos. Chem. Phys.*, 12, 3289-3310, 10.5194/acp-12-3289-2012, 2012.
- Ordóñez, C., Lamarque, J. F., Tilmes, S., Kinnison, D. E., Atlas, E. L., Blake, D. R., Sousa Santos, G., Brasseur, G., and Saiz-Lopez, A.: Bromine and iodine chemistry in a global chemistry-climate model: description and evaluation of very short-lived oceanic sources, *Atmos. Chem. Phys.*, 12, 1423-1447, 10.5194/acp-12-1423-2012, 2012.
- Plane, J. M. C., Joseph, D. M., Allan, B. J., Ashworth, S. H., and Francisco, J. S.: An Experimental and Theoretical Study of the Reactions $\text{OIO} + \text{NO}$ and $\text{OIO} + \text{OH}$, *J. Phys. Chem. A*, 110, 93-100, 2006.
- Saiz-Lopez, A., Plane, J. M. C., Mahajan, A. S., Anderson, P. S., Bauguitte, S. J.-B., Jones, A. E., Roscoe, H. K., Salmon, R. A., Bloss, W. J., Lee, J. D., and Heard, D. E.: On the vertical distribution of boundary layer halogens over coastal Antarctica: implications for O_3 , HO_x , NO_x and the Hg lifetime, *Atmos. Chem. Phys.*, 8, 887-900, 2008.
- Saiz-Lopez, A., Fernandez, R. P., Ordóñez, C., Kinnison, D. E., Gómez Martín, J. C., Lamarque, J. F., and Tilmes, S.: Iodine chemistry in the troposphere and its effect on ozone, *Atmos. Chem. Phys.*, 14, 13119-13143, 10.5194/acp-14-13119-2014, 2014.
- Sander, R.: Compilation of Henry's Law Constants for Inorganic and Organic Species of Potential Importance in Environmental Chemistry (v3), available at: <http://www.henrys-law.org/> (last access: 1 Sept 2016), 1999.
- Sander, S. P., Friedl, R. R., Golden, D. M., Kurylo, M. J., Moortgat, G. K., Wine, P. H., Ravishankara, A. R., Kolb, C. E., Molina, M. J., Diego, S., Jolla, L., Huie, R. E., and Orkin, V. L.: Chemical Kinetics and Photochemical Data for Use in Atmospheric Studies Evaluation Number 15, JPL_NASA, 06-2, Jet Propulsion Laboratory, Pasadena, CA, 2006.

Sander, S. P., Friedl, R. R., Barker, J. R., Golden, D. M., Kurylo, M. J., Sciences, G. E., Wine, P. H., Abbatt, J. P. D., Burkholder, J. B., Kolb, C. E., Moortgat, G. K., Huie, R. E., and Orkin, V. L.: Chemical Kinetics and Photochemical Data for Use in Atmospheric Studies, Evaluation No. 17, JPL_NASA, 10-6, Jet Propulsion Laboratory, Pasadena, CA, 2011.